Quaternary Science Reviews 30 (2011) 2626–2650

Contents lists available at ScienceDirect

Quaternary Science Reviews

journal homepage: www.elsevier.com/locate/quascirev

A high-resolution record of climate variability and landscape response from Kettle Lake, northern Great Plains, North America

Eric C. Grimm [a,*], Joseph J. Donovan [b], Kendrick J. Brown [c]

[a] Illinois State Museum, Research and Collections Center, 1011 East Ash Street, Springfield, IL 62711, USA
[b] West Virginia University, Department of Geology and Geography, Morgantown, WV 26501, USA
[c] Canadian Forest Service, 506 West Burnside Road, Victoria, BC V8Z 1M5, Canada

ARTICLE INFO

Article history:
Received 1 October 2010
Received in revised form
6 May 2011
Accepted 19 May 2011
Available online 29 June 2011

Keywords:
Northern Great Plains
Holocene drought
Endogenic carbonate precipitation
9.3 ka event
Aragonite
Pollen
Charcoal
Lake Agassiz
Ambrosia
Selaginella densa

ABSTRACT

A decadal-scale multiproxy record of minerals, pollen, and charcoal from Kettle Lake, North Dakota provides a high-resolution record of climate and vegetation change spanning the entire Holocene from the northern Great Plains (NGP) in North America. The chronology is established by over 50 AMS radiocarbon dates. This record exhibits millennial-scale trends evident in other lower-resolution studies, but with much more detail on short-term climate variability and on the rapidity and timing of major climatic shifts. As a proxy for precipitation, we utilize the rate of endogenic carbonate sedimentation, which depends on groundwater inflow, which in turn depends on precipitation. Independent cluster analyses of mineral and pollen data reveal major Holocene mode shifts at 10.73 ka (ka = cal yr BP), 9.25 ka, and 4.44 ka.

The early Holocene, 11.7–9.25 ka, was generally wet, with perhaps a trend to higher evaporation associated with warming temperatures. A switch from calcite to aragonite deposition associated with a severe, but brief drought occurred at 10.73 ka. From 10.73 ka to 9.25 ka, climate was generally humid but punctuated at 100–300 yr intervals by brief droughts, including the most severe drought of the entire Holocene at 9.25 ka. This event was coeval with the 9.3–9.2 ka event in the Greenland ice cores and observed at a number of sites worldwide. In contrast, the prominent 8.2 ka event in Greenland is not remarkable at Kettle Lake. The prominence of the 9.25 event locally in the NGP may be due to a major drawdown and northward retreat of Lake Agassiz at this time, reducing its mesoclimatic effect on the NGP and thrusting the region into an insolation controlled regime.

The mid-Holocene, 9.25–4.44 ka, was characterized by great variability in moisture on a multi-decadal scale, with severe droughts alternating with more humid periods. The high abundance of the weedy but drought intolerant *Ambrosia* generally during the mid-Holocene and specifically during the multi-decadal drought periods is seemingly paradoxical, but can be explained by high interannual variability of moisture overlaid on the multi-decadal variability.

The late Holocene, 4.44 ka–present, was also characterized by multi-decadal variability in moisture, but was generally wetter than the mid-Holocene and the magnitude of variability was less. The trends in wet-dry mineral, pollen, and charcoal proxies were similar to the mid-Holocene, but late Holocene mineral-pollen assemblages are distinct from mid-Holocene. The shift to wetter climate in the late Holocene was more gradual than the abrupt shift to arid conditions 9.25 ka, which may explain the asymmetric retreat and readvance of forest along the eastern margin of the NGP.

Precipitation variations in the NGP have been linked with Pacific and Atlantic sea-surface temperatures, and mid-Holocene drought in the NGP has been linked with sustained La Niña-like conditions in the Pacific. These linkages may explain the decadal- and millennial-scale variations seen in the NGP, but cause of the prominent century-scale variations remains elusive.

1. Introduction

The northern Great Plains (NGP) comprises the northern third of the vast grassland occupying the central portion of the North American continent. Both native vegetation and agricultural

* Corresponding author. Tel.: +1 217 785 4846; fax: +1 217 785 2857.
E-mail address: grimm@museum.state.il.us (E.C. Grimm).

0277-3791/$ – see front matter © 2011 Elsevier Ltd. All rights reserved.
doi:10.1016/j.quascirev.2011.05.015

production of the region are closely tied to its subhumid to semi-arid climate that is highly vulnerable to periodic drought (e.g. Woodhouse and Overpeck, 1998). Long-term ecological studies based on pollen records show dramatic changes in species composition in response to variation over time between drought and pluvial conditions (Albertson and Tomanek, 1965; Weaver, 1968; Lauenroth and Sala, 1992; Grimm, 2001). In addition to vegetation, the chemistry of lakes in the NGP is highly sensitive to moisture variations, albeit to greater or lesser degrees at individual lakes (Fritz et al., 1991; Laird et al., 1996b; Last and Ginn, 2005). In turn, these variations in chemistry influence the endogenic formation of various minerals (Last, 1993; Last and Sauchyn, 1993; Pienitz et al., 2000), which can be a coherent proxy of past climate, especially moisture balance. In this paper, we recognize the distinctions between endogenic minerals that precipitate from the water column, allogenic (detrital) minerals that originate from outside the lake basin, and authigenic minerals that result from diagenesis within the sediment (Jones and Bowser, 1978; Last, 2001; Last and Ginn, 2005).

The Holocene climate history of the NGP has long been generally understood based upon multiple lines of evidence. Gleason (1922) developed the idea of a "xerothermic" period in the Midwest, and Antevs (1955) popularized the concept of a more arid "altithermal" climate in the western United States during the mid-Holocene. After the advent of radiocarbon dating, studies in Minnesota east of the prairie-forest border showed that dry conditions prevailed during the mid-Holocene (~9–5 ka; ka = 1000 cal yr BP), resulting in the eastward expansion of prairie (e.g. Wright et al., 1963; McAndrews, 1966; Jacobson and Grimm, 1986), concurrent with a northward prairie expansion in Manitoba and Saskatchewan (e.g. Ritchie, 1964, 1976; Ritchie and Lichti-Federovich, 1968; Mott, 1973). Synoptic mapping of sites on the northern and eastern periphery of the NGP reveals the timing and pattern of early Holocene prairie expansion and late Holocene retreat (Bernabo and Webb, 1977; Webb et al., 1983). Prairie expanded eastwards from 11 to 7 ka, with the fastest movement 10–9 ka, and northwards from 12–10 ka. Thereafter, regional prairie retreat began ~6 ka, with the modern prairie-forest border becoming established ~2 ka (Williams et al., 2009).

The first pollen diagrams from the NGP were from sites along the eastern fringe in tallgrass prairie, including Pickerel Lake (Watts and Bright, 1968) and Medicine Lake (Radle, 1981; Radle et al., 1989) in eastern South Dakota and Lake West Okoboji in northwestern Iowa (Van Zant, 1979). These records show substantial sample-to-sample variability in pollen but have poor chronological control that is based on either few radiocarbon ages or ages on bulk sediment with old-carbon reservoirs (Kennedy, 1994). The only published accurately-dated NGP pollen diagram for the complete Holocene is from Moon Lake, southeastern North Dakota (Laird et al., 1996a, 1998b; Clark et al., 2001).

In addition to revealing millennial-scale changes in climate, many NGP sites also have the potential of yielding decadal- to century-scale records because they are characterized by rapid rates of sediment deposition together with minimal sediment mixing, coupled with the fact that several proxies such as pollen, charcoal, diatoms, ostracodes, geochemistry, and stable isotopes are highly sensitive to variations in moisture (Engstrom and Nelson, 1991; Fritz et al., 1994, 2000; Haskell et al., 1996; Laird et al., 1996a, 1998a, 1998b; Laird et al., 1996b; Valero-Garcés et al., 1997; Yu and Ito, 1999; Clark et al., 2001; Grimm, 2001; Clark et al., 2002; Last, 2002; Last and Vance, 2002; Smith et al., 2002; Yu et al., 2002; Laird et al., 2003, 2007; Umbanhowar, 2004; Brown et al., 2005). However, only a few high-resolution records have been developed, and all but one of these for only the late Holocene. These records include diatom-inferred salinity over the past 2300 years from Moon Lake (Laird et al., 1996b, 1998a); an ostracode-shell Mg/Ca proxy for salinity over the past 2100 years from Rice Lake, North Dakota (Yu and Ito, 1999); a multiproxy (geochemistry, pollen, and charcoal) record of moisture variability for the past 4500 years from Kettle Lake (Brown et al., 2005), a similar record for two short intervals centered on 8.2 ka and 2.8 ka from Kettle Lake (Clark et al., 2002), and a record of diatom-inferred salinity from Oro Lake, Saskatchewan for the past 7000 years (Laird et al., 2007). Many of these studies suffer from inaccurate chronologies based on few ^{14}C ages or bulk-sediment ages with unknown and often large old-carbon reservoirs (Grimm et al., 2009).

Here we report on a complete Holocene high-resolution record of sediment mineralogy, pollen, and charcoal from Kettle Lake, northwestern North Dakota. A pilot study by Clark et al. (2002) showed that geochemistry, pollen, and charcoal all responded to century-scale moisture variations during a ~600-yr interval centered ~8 ka. Indicators of moist conditions were aragonite, Poaceae pollen, and charcoal; whereas drought indicators were quartz and *Ambrosia*. This paper established some important associations of pollen and charcoal with moisture variations, which have since been observed at other NGP sites (e.g. Nelson et al., 2006). Importantly, in mixed-grass prairie, charcoal is a proxy for moister conditions inasmuch as charcoal production is dependent on fuel loads, which increase with increased moisture (Rogler and Hass, 1956; Whitman and Wali, 1975; Singh et al., 1983; Smoliak, 1986; Nelson et al., 2006). Brown et al. (2005) carried out spectral analyses of charcoal, Poaceae pollen, and carbonate estimated from loss-on-ignition from Kettle Lake for the past 4500 yr, which revealed a dominant 160-yr periodicity. Donovan and Grimm (2007) reported the episodic occurrence of struvite, an unusual guano mineral, in the mid-Holocene, which they hypothesized resulted from repeated visitations of large numbers of waterfowl when other lakes in the region were dry. Over most of the Holocene, sediments in Kettle Lake were (1) laminated (no bioturbation), (2) nearly continuous (no unconformities), and (3) aragonitic. Over 50 AMS radiocarbon dates on charcoal and terrestrial plant macrofossils provide a highly resolved and accurate age model. These data provide a detailed reconstruction of Holocene paleoclimate and landscape dynamics, including long-term trends, short-term variations, and the precise timing of modal shifts.

2. Site and regional setting

2.1. Kettle Lake

Kettle Lake (48°36.420′N, 103°37.446′W, 605 m a.s.l.) is located 43 km south of the US-Canada border and 31 km east of the North Dakota-Montana border (Figs. 1 and 2), in Williams County, North Dakota. The small modern lake (2.2 ha) lies within a roughly circular closed basin with water level ~10 m below the surrounding landscape. It lies in the drainage basin of the Little Muddy River, a south-flowing tributary to the Missouri River. It overlies the Little Muddy aquifer (Figs. 2 and 3), a glacial outwash sand and gravel deposit as thick as 35 m within the upper 50 m of glacial deposits (Witkind, 1959). As its name implies, the lake lies in glacial kettle, which is located near an esker channel trending NE-SW within a broad N–S trending glaciofluvial sediment sequence deposited near the end of the late Wisconsin glaciation (Witkind, 1959). The modern lake, which was 10.2 m deep in 1996, has a simple bowl-shaped morphometry. The lake is one of the deepest in a region spotted with thousands of shallow "prairie potholes." The climate is semiarid (320 mm/year annual precipitation); most of the water and nearly all solutes entering the lake are derived from groundwater inflow.

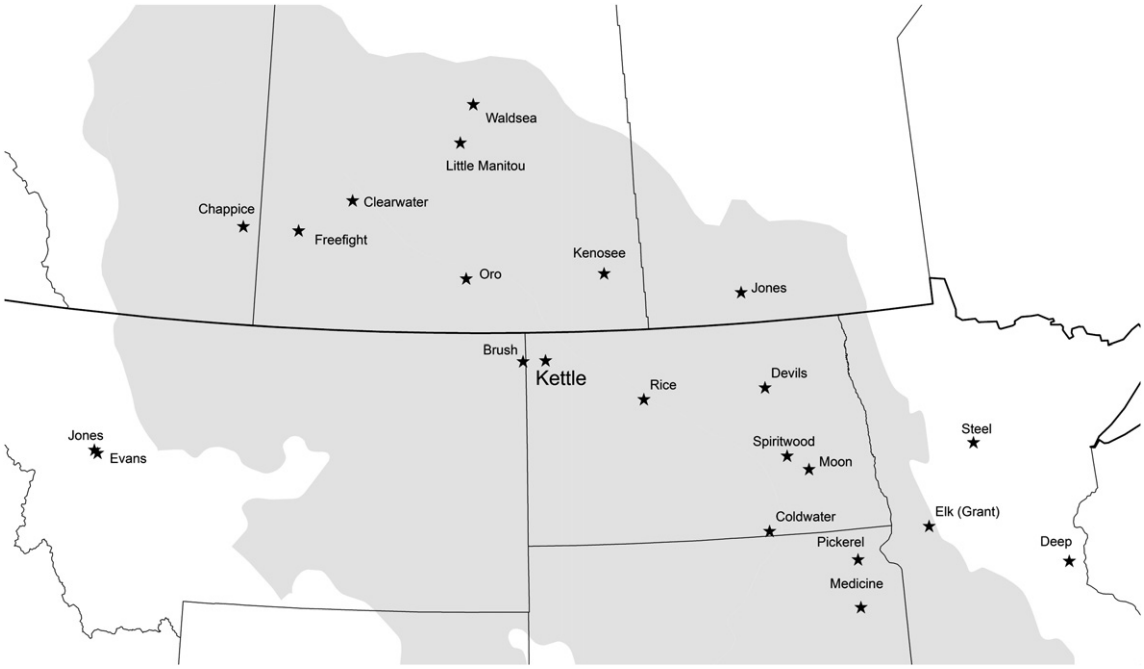

Fig. 1. Location of Kettle Lake and other NGP sites with Holocene paleoclimate records. Shaded area represents the Great Plains division of North American ecoregions (USEPA, 2006; http://www.epa.gov/wed/pages/ecoregions/na_eco.htm).

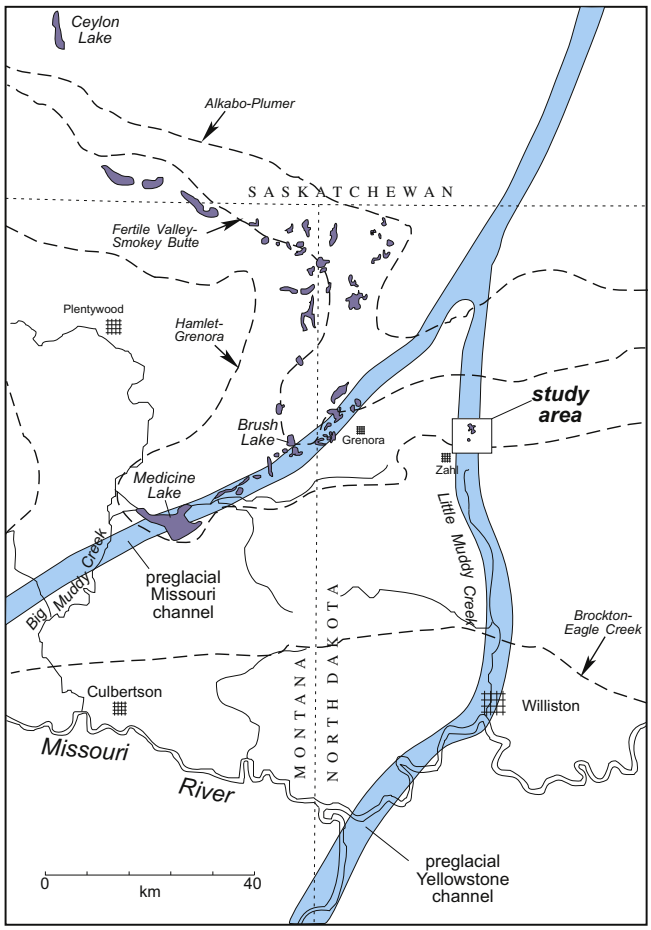

Fig. 2. Regional Late Wisconsin ice-recessional positions and preglacial buried fluvial channels in the Kettle Lake region, after Witkind (1959), Hansen (1967), and Clayton et al. (1980).

Kettle Lake is of special interest for a number of reasons: (1) it is actively producing endogenic carbonate from a groundwater source, and has done so throughout the Holocene; (2) local groundwater conditions are known with some precision; (3) it is sufficiently deep to have never gone dry or deflated in the Holocene; and (4) its simple morphometry suggests that patterns

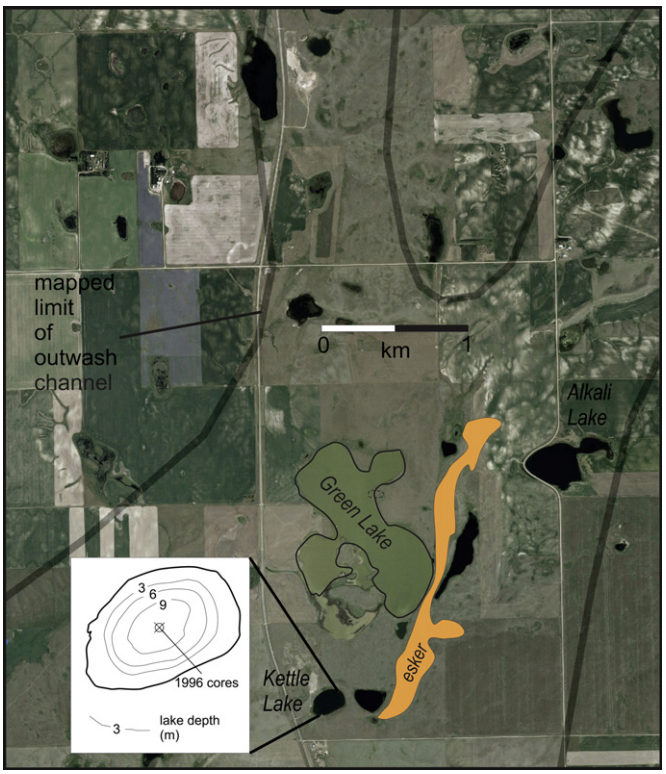

Fig. 3. Aerial photo of Kettle and surrounding region. Outwash channel limits after mapping by Witkind (1959).

of sedimentation and groundwater inflow/outflow are reasonably simple in contrast to some other investigated NGP lakes, e.g., Rice Lake and Coldwater Lake (Fritz, 1996; Fritz et al., 2000; Laird et al., 2003). Hydrologically, the lake has no perennial or ephemeral surface-water inflow or outflow. Thus the only possible surface-water inflow is slopewash that may enter the lake from the small catchment during intense rain or snowmelt events. However, because the lake basin lies in highly permeable outwash, slopewash is minimized. Lake water is currently unusually low in dissolved solids (<2000 mg/L) compared to other lakes of this region, which have salinities up to 240,000 mg/L, owing to a high rate of surface evaporation (Last, 2002; Donovan and Grimm, 2007). Its salinity is similar to that of the dilute, hard groundwater in the outwash aquifer beneath and surrounding the lake. Groundwater from numerous subaqueous springs along the lake margin is the primary water supply for the lake (Donovan and Grimm, 2007, Table 1). Lake water is only slightly higher than source groundwater in Na, Mg, SO_4, and Cl, and is fairly similar in Ca and alkalinity. This dilute water chemistry is consistent with endogenic $CaCO_3$ production in the lake (pH 8.7–8.9) with relatively minor evaporative concentration of other solutes, in comparison to many surrounding lakes. The low salinity suggests that the hydraulic residence time of water in the lake is brief and that Kettle Lake is very much a "flow-through" lake.

Kettle Lake lies within the mixed-grass prairie (Weaver and Albertson, 1956; Whitman and Wali, 1975; Coupland, 1992). The dominant grasses are *Pascopyrum smithii*, *Bouteloua gracilis*, *Koeleriapyramidata*, and *Hesperostipa comata*. In addition to grasses, the mixed prairie contains a diversity of forbs. The Asteraceae, Fabaceae and Amaranthaceae are particularly important. A number of *Artemisia* species occur, and *Artemisia frigida* is the most important forb in the northern mixed-grass prairie (Coupland, 1950, 1992). Taxonomic nomenclature follows Flora of North America (Flora of North America Editorial Committee, 1993+), except for Amaranthaceae, which follows the Angiosperm Phylogeny Group (Stevens, 2001 onwards; Angiosperm Phylogeny Group, 2009), wherein the Chenopodiaceae have been synonymized with the Amaranthaceae.

2.2. Late Pleistocene history

Kettle Lake lies within the bedrock channel of the preglacial north-flowing Yellowstone River, which along with the preglacial Missouri flowed northeast into Hudson Bay (Hansen, 1967; Freers, 1970). Glacial outwash tends to be localized in these preglacial channels. Kettle Lake lies in deepest part of the channel, where depth to bedrock is ~140 m. Pleistocene channel fills include till, outwash, and lake sediments (Witkind, 1959). These late Wisconsin deposits are a complex assemblage of collapsed outwash, end moraines, dead-ice moraines, lake sediments, eskers, disintegration ridges, and meltwater channels (Hansen, 1967; Freers, 1970). At its southernmost advance to the Brockton-Eagle Creek (Howard, 1958) or Long Lake (Clayton et al., 1980; Bluemle et al., 2004) positions, late Wisconsin ice extended to near or beyond the Missouri River, well south of Kettle Lake. Although not well dated, the estimated age of this advance is ~20 ^{14}C ka (24 cal ka) (Clayton et al., 1980; Clayton and Moran, 1982). After receding from the maximum late Wisconsin position, ice readvanced to or had recessional still-stands at several positions from near Kettle Lake and successively north to the Hamlet-Grenora, Fertile Valley-Smokey Butte, and Alkabo–Plumer positions (Hansen, 1967) (Fig. 2). The estimated age of the Hamlet-Grenora advance, which extended just south of KettleLake, is ~15 ^{14}C ka (18 cal ka). The Fertile Valley-Smokey Butte position north of Kettle Lake may correspond to the North Dakota Phases F-G-H (14–13 ^{14}C BP; 17–16 cal ka). The Alkabo–Plumer position may correspond to North Dakota Phase I (12.3 ^{14}C ka; 14.1 cal ka). From the Alkabo–Plumer position, ice retreated into southern Saskatchewan and did not return to the region (Clayton and Moran, 1982). Thus, based on current chronology, Kettle Lake was deglaciated sometime between 18 ka and 16 ka.

As ice retreated from Zahl to the Alkabo–Plumer position (~14.1 cal ka), glacial meltwater carried outwash sediment into the south-flowing drainage of the Little Muddy valley, at a time in which dead-ice blocks and features were likely extensive across the landscape and, in particular, within the outwash channel complex of the Little Muddy. These outwash sediments buried blocks of remnant ice, one of which later melted out to form Kettle Lake as well as many other lakes within the channel. The basal age of the Kettle Lake sediments is ~13.0 ka (Grimm, 2011). Thus, 1100–1500 years elapsed between the Alkabo ice stand and the first accumulation of sediment in Kettle Lake.

2.3. Hydrology

In addition to Kettle Lake, a number of other lakes and wetlands overlie the Little Muddy aquifer. Some are relatively fresh whereas others (Green Lake, Alkali Lake; Fig. 3) are saline. We infer that the fresh lakes have relatively equal inflow and outflow, i.e. are "flow-through" lakes; whereas the saline lakes lie on clayey till or lacustrine deposits with low permeability. Kettle Lake lies in highly permeable sand and gravel outwash, which is exposed in several gravel quarries near the lake and which contribute to its flow-through nature, in contrast to nearby saline lakes. The Little Muddy aquifer (Fig. 3) extends from the Hamlet-Grenora ice position south to near Williston. It is composed of an upper gravel zone of highly permeable outwash and lower gravel zone of valley-fill preglacial alluvial deposits, but only the upper outwash deposits interact with lakes. The aquifer is from 3 to 8 km wide. The thickest outwash is up to 28 m in the center of the aquifer, but is only about 15 m thick in the vicinity of Kettle Lake. Groundwater in the Little Muddy aquifer flows from north to south at a hydraulic head gradient of about 4 m per kilometer (file data, North Dakota State Water Commission).

Major ions of Kettle Lake water are Mg, Na, and HCO_3 with relatively low total dissolved solids (TDS) (1.6 g/L average) and pH 8.2. Aquifer groundwater is even more dilute, with major ions Ca-Mg-HCO_3 and 0.5–0.7 g/L TDS. The lake is about 3 times more concentrated in dissolved solids than aquifer groundwater in the lake vicinity. The lake, however, is much lower in calcium (18–29 mg/L vs. 110–172 mg/L), including groundwater entering the lake sampled from the lake bed. The increase in lake-water salinity is attributed to evaporation of lake water, and the decrease in lake-water calcium to precipitation of carbonate minerals in the lake. Water chemistry data for Kettle Lake and surrounding wells in the aquifer are given in Donovan and Grimm (2007).

3. Methods

3.1. Core handling and photography

In July 1996, two overlapping cores recovering nearly 22 m of sediment were taken from near the center of the lake with a 5-cm diameter Wright square-rod piston corer (Wright et al., 1984). The cores were taken from raft fixed in position by a rope stretched across the lake and by two large anchors set at right angles to the rope. Two cores, labeled “A” and “B”, were taken, spaced ~1 m apart. Individual core drives were generally 1 m long; drive depths were offset vertically by 50 cm between the A and B cores. The mud–water interface was at 10.20 m depth below lake level, and the maximum core depth was 32.07 m below lake level. Both cores were split lengthwise to enable imaging, stratigraphic description, and sampling. The

unoxidized sediment was dark gray to black, with little apparent structure. However, after the cores oxidized in a cold room (4 °C) for about 90 days while still wrapped in plastic and foil, they developed substantial coloration and contrast, with horizontal laminations clearly visible from top to bottom. The oxidized splits were photographed in 15-cm increments with color print film. These prints were scanned at 600 dpi and digitally stitched into single images for each core drive at 1:1 scale. The laminations facilitated accurate stratigraphic correlation between the A and B cores, and a complete composite image was constructed for the entire sedimentary sequence. Sections of this image were taken from either core A or core B depending on core lengths and recovery.

Detailed correlation of the overlapping cores indicated complete sediment recovery. Missing sections in either core were spanned by the other core; however, equivalent sections in the two cores varied in thickness, and the total composite core length is less than the depth cored, thus indicating compression. We believe that the most likely explanation for this compression is that either water or sediment was squeezed to the side as pressure from the partly filled core barrel was applied from above. The digital images of the composite core were sliced into nominal 4-cm sections (4 times the recovery proportion of the relevant core section), which were then stretched to exactly 4 cm using imaging software. These stretched core images were re-stitched into 1-m sections and printed at 1:1 scale. Thus, linear measurements taken from these images with a meter scale correspond to the original core depths. The final digitized images were marked with 1-cm tic marks, and these marks were used as a guide for slicing the cores into nominal 1-cm segments, nominal because the actual thicknesses did not necessarily correspond with the 1-cm divisions on the stretched digital image. The individual slices were taken from either core A or B, but not both; and the overlapping, unsliced core was retained as an archive.

The 1-cm sediment slices were stored in labeled vials, and subsamples for all proxies (pollen, charcoal, diatoms, LOI, and mineralogy) were extracted from these vials with a volumetric cylindrical sampler. Thus, accurate depth correlation between proxies was ensured. Larger volumes of sediment required for recovery of plant macrofossils and charcoal for AMS ^{14}C dating were taken from the unsliced archive core. For this sampling, stratigraphic correlation was made by visual comparison of the unsliced core with the photographic images of the sliced core, aided by the unique lamination sequences. Pure lenses of mineral separates were handpicked from the core and stored separately.

3.2. Quantitative mineralogy

Bulk-sediment samples from the 1-cm intervals and one split of the hand picked mineral separates were analyzed by powder XRD techniques. Both were oven dried at 80 °C, then pulverized with an agate pestle to fine (<100 mesh) size. The powders were mounted on 3-mm thick 45-mm diameter Chemplex® disks, for analysis by X-ray diffraction using Ni-filtered Cu-Kα radiation on a Panalytical® Xpert Pro diffractometer. The X-ray detector employed was an Accelerator®, which speeds collection of the sample reflections by a factor of 6–10 over conventional detection. Samples were scanned for approximately 30 min from 5° to 75°2 theta. Phases were identified using Panalytical® Xpert Highscore© search-match software and the PDF-2 dataset (2003). For a few mineral-separate samples of limited volume that only thinly covered the mounting plate, care was taken to identify and discount peaks of the Chemplex medium at d-spacings 8.45, 5.16, 4.70, 4.25, 3.86, and 3.19 Å, easily recognized visually according to their location and broad shape. The bulk samples were calibrated with pure mineral standards in specified mass/mass ratios to a pure quartz reference phase. Peak height above background for specific diagnostic peaks for each mineral phase were averaged and employed using a linear standard curve to estimate quantitative percentage of aragonite, quartz, dolomite, calcite, muscovite, chlorite, amphibole (hornblende), albite, and orthoclase, as a percent of the crystalline fraction. Results were calculated according to the matrix flushing method (Chung, 1974), using quartz as a reference. Struvite (Donovan and Grimm, 2007), also present in approximately 35 of the core slices, was identified by XRD but only as pure crystalline phases and therefore not included in the quantitative analysis of sediment.

The resulting XRD percentages represent semi-quantitative mass percent of the crystalline fraction of each core slice, at 1-cm increments. The term "semi-quantitative" refers to the fact that, even in mineral mixtures for which all unknown phases have accurate standard calibration, there are uncertainties induced due to factors such as calibration, interpretive, and random errors (Till and Spears, 1969). Random errors may relate to either sample condition/preparation, sample mounting, or instrument error and include preferred mineral orientation, grain size of mineral phases, accurate focusing of the beam at the sample surface, and sample thickness. In polymineralogic mixtures, these errors may be exaggerated by accumulation of error from multiple minerals; the potential for interference/overlap between diagnostic peaks of specific minerals and any peaks from other minerals; and other factors. In general, accuracy of XRD is best for relatively abundant minerals with unambiguous strong diagnostic peak locations unsusceptible to interference with peaks of other minerals. Several of the minerals in this investigation (quartz, aragonite, calcite, dolomite, clay minerals, and, to a lesser degree, gypsum, which is low in abundance) meet these criteria. Other minerals (feldspars and amphibole) are generally less abundant or in trace concentrations and therefore less accurately determined; additionally, there is a rich variety of minerals in these groups, and the potential for confoundment in identification is greater than for other minerals. These latter minerals are therefore lumped together in a "silicates" category. Although these XRD results are semi-quantitative, their variations may be determined to high sensitivity, even if absolute accuracy is not high.

3.3. Pollen, LOI, charcoal, and radiocarbon analyses

Samples for pollen analysis were prepared with standard procedures (Fægri et al., 1989) and mounted in silicone oil. Pollen sums of at least 300 upland types were counted by E.C. Grimm, B.C.S. Hansen, and I. Stefanova. Only seven dominant pollen taxa, which generally comprise 80–90% of the pollen sum, are presented in this paper. Some of these taxa are designated as a -type or undiff. (undifferentiated). These are so labeled on the figures, but for ease of discussion the -type or undiff. suffix is left off in the text. Amaranthaceae undiff. excludes *Salsola*, which is morphologically distinctive. Asteroideae is a subfamily of the Asteraceae, and Asteroideae undiff. excludes the subtribe Ambrosiinae (*Ambrosia*, *Iva*, *Xanthium*) and *Artemisia*, which are recognizable pollen types. *Ambrosia*-type includes *Iva axillaris* as well as *Ambrosia*. *Selaginella densa*-type includes *S. densa* and *S. rupestris*, however *S. densa* is the only common species of *Selaginella* in the NGP, where today it may rival grasses in coverage (Coupland, 1950; Hall-Beyer and Gwyn, 1996). *S. densa* is common around Kettle Lake today.

Volumetric samples (0.5 ml) for loss-on-ignition analysis (Dean, 1974) were dried overnight at 100 °C, weighed, and ignited at 500 °C for 1 h, weighed, ignited at 900 °C for 1 h, and weighed. Samples were cooled in a desiccator. Controls of ash-free filter paper and laboratory grade $CaCO_3$ were run with each batch to check for complete burn of organic matter at 500 °C and complete dissociation of $CaCO_3$ at 900 °C.

To reconstruct the incidence of past fire, charcoal fragments were sieved from 0.5 ml subsamples from the 1-cm slices. Samples

were gently sieved through a 180 μm screen, and the coarse fraction retained was examined for charcoal under a dissecting microscope at 20× magnification. The microscope was fitted with a video mount and the charcoal fragments analyzed using *NIH IMAGE* software to measure length, width, and total area. Charcoal flux ($mm^2 \cdot cm^{-2} \cdot yr^{-1}$) was determined for each sample by multiplying charcoal concentration ($mm^2 \cdot cm^{-3}$) by the vertical accretion rate ($cm \cdot yr^{-1}$) from the age model, followed by a square root transformation to minimize the variance.

Plant macrofossils and charcoal for AMS radiocarbon dating were sieved from 1-cm slices of the archive core. If suitable materials but in an insufficient quantity were found in a sample, additional 1-cm slices were added until an adequate quantity of material was recovered. Terrestrial macrofossils were scarce throughout much of the core, and most of the samples for radiocarbon dating were charcoal. Initially, core sections targeted for dating were sieved until sufficient charcoal was obtained for a date. Samples were first treated with 10% HCl, which disaggregated the carbonate-rich sediment and removed carbonate adhering to charcoal and macrofossils. Sediment was then gently screened through a stack of 0.42 mm, 0.2 mm, and 0.15 mm sieves. Charcoal and macrofossils were picked with forceps under a stereomicroscope. Picked samples were re-picked at least twice to remove all sediment residues from the charcoal and macrofossil samples. Charcoal samples typically consisted of 10 to >100 fragments. Charcoal and macrofossil samples were stored in distilled water with a few drops of 10% HCl to acidify and prevent fungal growth. The wet samples were submitted to the Center for Accelerator Mass Spectrometry (CAMS) at Lawrence Livermore National Laboratory for dating.

3.4. Numerical analysis

Mineral, pollen, and charcoal data were subjected to cluster analysis by the method of incremental sum-of-squares (Ward's method) with the CONISS program (Grimm, 1987). Three different cluster analyses were performed: separate stratigraphically constrained cluster analyses of the (1) pollen and (2) mineral data and (3) a stratigraphically unconstrained analysis of the combined pollen and mineral data. The pollen data included 35 pollen types having percentages of at least 1% in one sample. The mineral data included the 6 most abundant minerals or mineral classes (quartz, aragonite, calcite, dolomite, gypsum, and "other silicates", including summed amphibole, feldspar minerals, kaolinite, chlorite, and muscovite). Percentage values were used after the pollen and mineral data were re-summed to 100%. For the combined analysis, all variables were standardized to mean zero, SD 1, and therefore weighted equally in the analysis. Because standardization magnifies the noise in uncommon variables, the pollen dataset was reduced to 8 abundant types: *Picea*, *Ambrosia*, *Artemisia*, Asteroideae, Amaranthaceae, Poaceae, *Salsola*, and *S. densa*. The same 6 mineral variables as in the constrained analysis were used. Because this unconstrained analysis is independent of time and depth, the clusters are comprised of samples with similar sediment mineralogy and pollen assemblages that are not necessarily adjacent.

Principal Component Analysis (PCA) was carried out on a joint dataset of minerals, pollen, and charcoal using the correlation matrix. The suite of mineral and pollen variables was the same as the joint cluster analysis with the addition of charcoal. The most revealing analyses were those carried out separately on the mid-Holocene and late Holocene zones identified by the cluster analyses.

4. Aragonite as a quantitative measure of moisture balance

A relatively new proxy for precipitation is the rate of endogenic carbonate sedimentation (Shapley et al., 2005). In some alkaline lakes, carbonate deposition is derived almost exclusively from groundwater inputs of Ca and alkalinity. Although carbonate minerals in lake sediment may be either allogenic or endogenic (Last and Ginn, 2005), aragonite is solely endogenic as virtually all $CaCO_3$ in rocks and sediments older than Pleistocene is calcite (Larsen and Chilingar, 1967), whereas calcite may be allogenic or endogenic (Last and Ginn, 2005). Thus, if the endogenic phase of $CaCO_3$ is aragonite, discrimination of endogenic from detrital carbonate is possible. Aragonite precipitation in alkaline lakes and in seawater is favored by a high ratio of Mg to Ca (Folk, 1974; Kelts and Hsü, 1978; De Choudens-Sánchez and González, 2009). In NGP lakes, aragonite precipitation occurs mainly in summer because of photosynthetic uptake of CO_2 and the resultant increase in pH (Last and Ginn, 2005).

Shapley et al. (2005) showed that during the 20th century, endogenic carbonate flux (ECF) of aragonite in sediments of two western Montana lakes (Evans and Jones, Fig. 1) correlated with instrumental climatic humidity. They interpreted the causal mechanism as the rate of groundwater inflow and associated solute delivery to the lake. Evans Lake, which was more saline and had lower mean Ca concentration (4.1 mg/L) than Jones Lake, provided the stronger correlation, suggesting the correlation is most appropriate for lakes in which carbonate precipitation is Ca limited. Despite this evidence, questions remain as to which lakes produce carbonate sediment according to this process and how persistent and reliable carbonate flux might be as a proxy for drought (or precipitation).

Modern Kettle Lake has lower salinity and higher Ca than either Jones or Evans Lakes (Donovan and Grimm, 2007). During the 20th century, both endogenic carbonate flux (ECF) and detrital mineral flux (DF) were calculated for a ^{210}Pb-dated record from Kettle Lake (Donovan et al., 1999). In this record, the 1925–1937, 1953–1961, and post-1981 droughts were recorded as ECF declines, indicating that aragonite precipitation correlates with humidity cycles. Also observed were large abrupt DF spikes in the 1950s and 1960s that were clearly unrelated climate cycles, but most likely emanated from a gravel pit located immediately north of Kettle Lake (Donovan et al., 1999). Nonetheless, concentration of aragonite in Kettle Lake sediment is correlated with modern precipitation and with other climate-sensitive proxies prior to modern anthropogenic influence; and a relationship clearly exists between precipitation and aragonite flux. Clark et al. (2002) observed strong cyclicity in aragonite, pollen, and charcoal at Kettle Lake within a 600-yr-long interval centered at ~8.0 ka. High aragonite concentrations correlated with high Poaceae, high charcoal, and low *Ambrosia*, as well as low benthic diatoms. Brown et al. (2005) demonstrated that a similar pattern prevailed throughout the late Holocene (0–4.5 ka).

Sections of the Kettle Lake core are laminated light-dark couplets, which probably are annual (varves). However, these sections are sufficiently discontinuous or difficult to identify that traditional varve counting for chronology would be unproductive. If varves could be identified and measured in thickness, they might be employed to estimate groundwater inflow rate, which equates to cumulative groundwater recharge over the subsurface catchment supplying the lake:

$$Q_{in} = \frac{C_{arag} n_x h_{varve} A_{lake}}{Ca_{gw} - Ca_{lake}}$$

where

Q_{in} = groundwater inflow rate per year
C_{arag} = molar volumetric concentration of aragonite in an annual layer
Ca_{gw} = molar dissolved Ca concentration in groundwater inflow

Ca_{lake} = molar dissolved Ca concentration in lake water
n_x = mineral fraction as percentage of bulk sediment
h_{varve} = annual sediment accumulation (thickness)
A_{lake} = area of lake sedimentation

To be sure, there may be uncertainties in estimating several of these parameters due to spatial or temporal variability; and to apply this relationship, sediment observations from multiple locations in the lake would be required. Similarly, laminated couplets in the core would have to be unambiguously demonstrated to be annual. Nevertheless, this equation quantifies the relationship between groundwater inflow rate and aragonite concentration, and it may provide a useful tool in relating sedimentary carbonate concentrations quantitatively to catchment water budget. Similarly, it implies that carbonate-poor intervals (dark layers common in the Kettle Lake mid-Holocene) may well represent long periods of low groundwater inflow, e.g. long droughts.

5. Sediment description

Most of the Kettle Lake sediment is finely laminated silty carbonate mud or silty diatomaceous ooze (as per Schnurrenberger et al., 2003) (Fig. 4). The laminations form a repetitive sequence of light–dark rhythmites some of which are probably annual (i.e. varves), but rhythmite counts assuming annual laminations in the upper part of the core (1020–~1565 cm) by three different investigators resulted in widely different age-span estimates, none of which corresponded to that from radiocarbon dates. Microscopic examination showed that some light-colored laminations in the upper part of the core are diatomite, whereas others are carbonate. Below ~1565 cm, light-colored laminations are principally carbonate.

Interbedded with the laminated sediments are several coarsely-banded or chaotically-bedded "slump" units (shown by black bars in Fig. 4). Although we use the term "slump" for these strata, as is common in the limnological literature (e.g. Bennett, 1986), these strata may not be true slumps with rotational movement but rather slides, plastic flows, or turbidites (Mulder and Cochonat, 1996), or they may have resulted from in-place soft-sediment deformation, or some combination of these processes. The origin may not be definitively determined without additional information describing the extent and geometry of the deformation, such as seismic profiles or additional cores.

The slumps occur in three stratigraphic groups (Figs. 4 and 5). The first group consists of a large slump,unit with an underlying folded structure. A unit 156-cm thick, hereafter called the "big slump", with sharply defined lower and upper contacts at 2514 cm and 2358 cm, is massive, locally convolute, and visually distinct from the regularly-laminated sediments above and below. This interval contains irregularly-deformed horizontally banding that may be correlated between the two cores. Abundant littoral plant macrofossils (especially *Schoenoplectus* and *Chenopodium* seeds) suggest that this sediment was originally deposited in shallower water and later transported into the deeper portion of the basin. The slump is bracketed by two ^{14}C ages in undisturbed sediment of 6365 ± 40 ^{14}C yr BP (95% range: 7.419–7.248 cal ka) on charcoal 7 cm above the slump (2349.5–2352.5 cm) and 6720 ± 35 ^{14}C yr BP (95% range: 7.662–7.512 cal ka) on *Cenchrus longispinus* (sand bur) seeds immediately below the slump (2514.5–2515.5 cm). The time interval between the medians of the calibrated bracketing ages is 283 yr, and according to the age model (described below) the time interval between the upper bracketing date and the top of the slump is 20 yr. Thus, the estimate for the missing section of sediment is ~260 yr (Grimm, 2011). The sudden slumping of 1.5 m of sediment would have disturbed the watery, unconsolidated surficial sediments, and the appearance of a hiatus in the record is therefore not surprising. Based on the deposition time of sediment below the slump, the gap in the sedimentary sequence is estimated to be ~43 cm. A folded structure 46 cm below the big slump (2571–2560 cm) appears to be the result of soft-sediment deformation of the type commonly attributed to seismic events (Seilacher, 1984; Becker et al., 2005) or rapid loading and liquefaction, rather than a block or slab failure, as undeformed laminae in one core can be traced to folded laminae in the other.

The second group of three slump deposits occurs at 2657–2669 cm, 2686–2700 cm, and 2717–2780 cm dating to the early Holocene/mid-Holocene transition, ~9.3–8.8 ka (Figs. 4 and 5). These slumps appear to represent three discrete units with intact finely laminated primary sediment between them. The slump material is variable in texture, ranging from sand to clay, and may represent a diamicton of allochthonous littoral sand and lake sediment. A distinctive slump block with laminated lake sediment lying at ~45° occurs at 2772–2779 cm (Fig. 4).

The third group of slump deposits occurs in the basal sediments at 2981–3010 cm, 3058–3081 cm, 3090–3106 cm, and 3109–3125 dating to ~12.68–11.6 ka. These deposits are diamictons of sand and lake sediment as in the second group. Two radiocarbon dates from the uppermost of these deposits are much older than dates from bracketing lake sediments. These dates of 13,080 ± 45 ^{14}C yr BP (95% range: 16.413–15.215 cal ka) and 29,230 ± 230 ^{14}C yr BP (95% range: 34.566–33.267 cal ka) are on wood charcoal (Grimm, 2011), suggesting that this material had an allochthonous origin. The total depth of the small lake basin is over 40 m, and successive flows of sand may have occurred as buried ice continued to melt or oversteepened slopes collapsed.

To assemble a stratigraphic sequence of primary sediment only, the slump intervals were removed, leaving a composite core with a nearly continuous sedimentary record. Recognition of these discordant intervals would have been difficult or impossible without laminated sediments and a large number of radiocarbon dates. In fact, because the structure and bedding of the slumped sediments are not, in general, highly deformed, the discordant intervals were only confirmed when radiocarbon ages indicated inversions. Thus, without obvious sediment lamination and a large number of accurate well-calibrated ^{14}C age dates, many or most of the discordancies could well have gone unrecognized.

6. Age model

Chronology of the Kettle Lake sediments is based on 53 AMS radiocarbon dates (Fig. 5), all except one obtained from terrestrial plant macrofossils or charcoal. Grimm (2011) describes the details of the age model and lists the uncalibrated and calibrated radiocarbon dates. Radiocarbon ages were calibrated and tested for outliers with the program BCal (Buck et al., 1999), available from http://bcal.sheffield.ac.uk, using the IntCal09 calibration curve (Reimer et al., 2009). BCal uses Bayesian statistics with an option for an *a priori* assumption that dates higher in the core are younger than ages lower in the core. When ages with overlapping calibrated probability distributions occur, BCal produces posterior probability distributions with non-overlapping modes, essentially wiggle-matching the ages to the calibration curve. Outlier analysis is an option within BCal. Ages were also calibrated with Calib (Stuiver and Reimer, 1993), which makes no stratigraphic assumptions. These ages were used to help evaluate stratigraphically reversed radiocarbon ages.

Eight ages were rejected as outliers *a priori*. One of these ages was on a sample of nonspecific organic detritus, presumably from aquatic marcrophytes (CAMS-38086, 2680 ± 100 BP). A charcoal

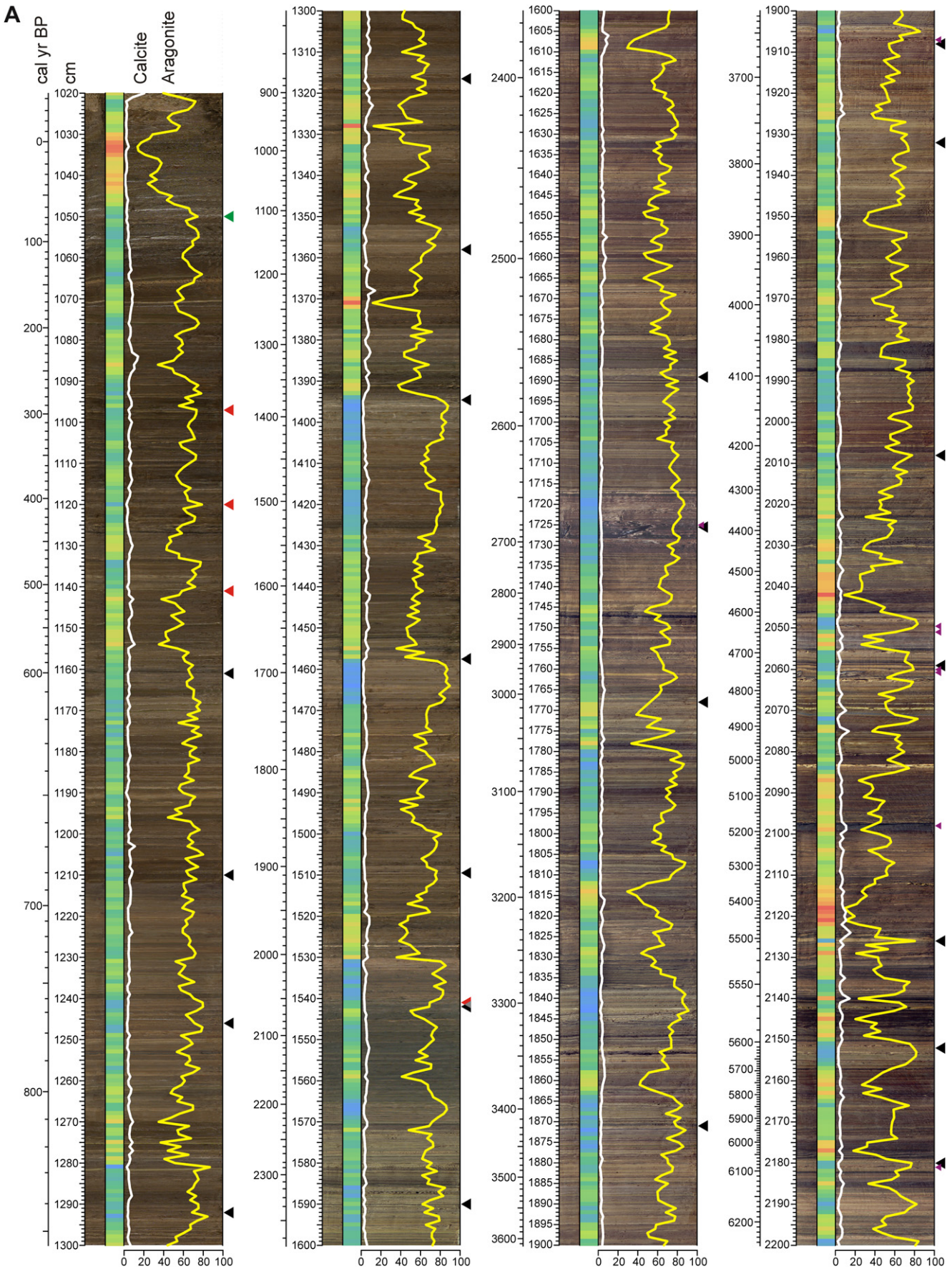

Fig. 4. Laterally-stretched core images (5×) with superimposed aragonite and calcite percentages (yellow and white lines, respectively). Core images are also shown to scale, separated by a color scale keyed to aragonite values, as a proxy for groundwater inflow and precipitation. Color-indexed carets indicate accepted and rejected ^{14}C ages; location of the *Salsola* rise, and struvite mineral occurrences.

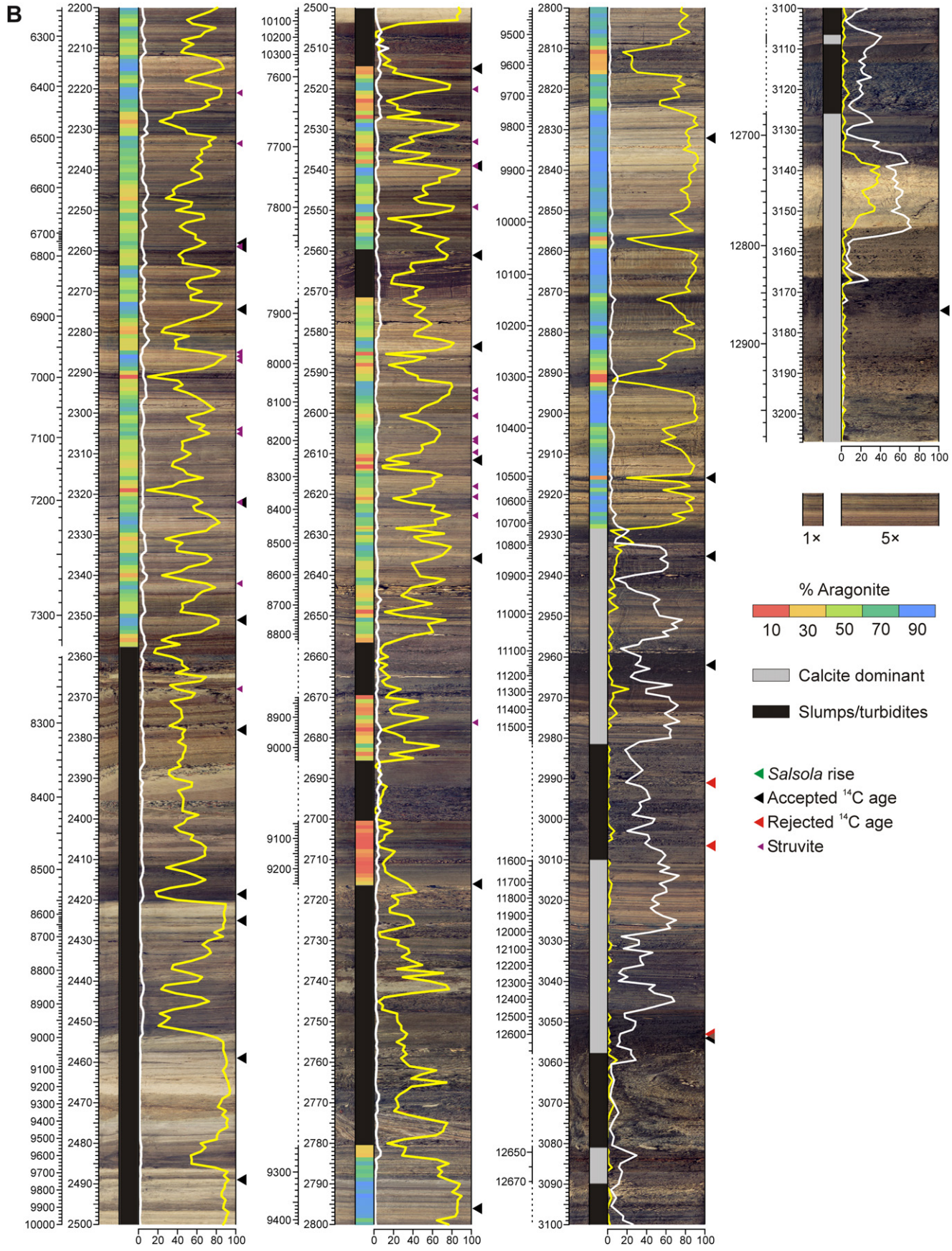

Fig. 4. (*continued*).

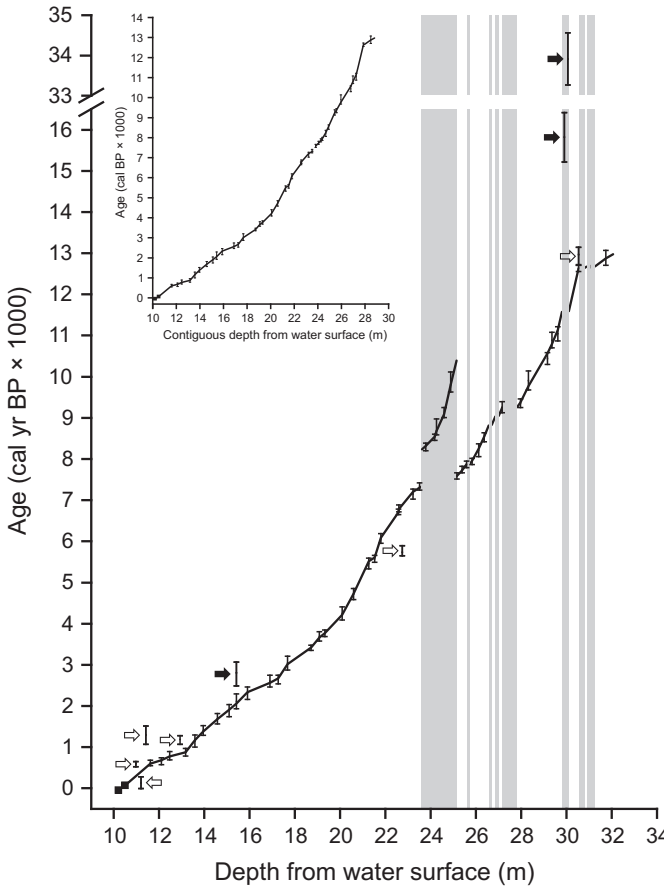

Fig. 5. Age model for Kettle Lake expressed as calendar years vs. depth, showing non-conformable slumped intervals (vertical gray bands), 95% ranges of calibrated ^{14}C ages, and reconstructed age-depth curve (inset). After Grimm (2011).

sample from the same level is 600 ^{14}C yr younger (CAMS-38087, 2080 ± 50 BP), which shows the magnitude of the hardwater error. Two of the rejected ages are from a sand layer near the base of the core (2981–3010 cm) and are reversed relative to bracketing ages and are probably on redeposited materials. The older of these two ages (29,230 ± 230 BP, CAMS-113587) is clearly too old based on regional glacial geology (Clayton and Moran, 1982); however, the younger of these ages (13,080 ± 45 BP, CAMS-113586) is not implausibly old and might have been accepted if not for other younger bracketing dates. The remaining five ages rejected *a priori* as outliers are from the big slump.

Six additional radiocarbon ages were rejected as outliers based upon the BCal outlier analysis or on a more stringent criterion applied to statigraphically reversed radiocarbon dates than that applied by the BCal: reversed dates were not accepted if their 2σ ranges as determined by Calib did not overlap stratigraphically adjacent dates. The rationale for this more stringent criterion is that the BCal assumes that ages stratigraphically higher in the sequence must be younger than deeper ages, as outer tree rings must be younger than inner rings. However, plant macrofossils have potential taphonomic complications, and the age of the macrofossil is not necessarily the age of deposition. The BCal outlier analysis will likely not identify redepostion of materials only a few decades to a few hundred years older than the date of sedimentation; hence, the more stringent criterion adopted here (Grimm, 2011).

A final BCal run on the final set of 39 accepted ^{14}C dates produced a series of calibrations with monotonically increasing median probabilities with depth (Fig. 5). An age model was developed from this series of calibrated dates by linear interpolation between the calibrated medians. With so many dates, fitting a smoothed curve, such a spline, results in very little difference from the linear model in the interpolated ages between dates. Slump deposits were removed, and contiguous depths were assigned before developing the age model. Estimated ages were not assigned to sediments within these smaller sections of redeposited sediments.

7. Results

7.1. Cluster and PCA analyses

Based on the results of the three cluster analyses (Figs. 6 and 7, Fig. S1), we designate six stratigraphic zones, labeled A–F (Fig. 8). Zone boundaries are placed at 11.93 ka, 10.73 ka, 9.25 ka, 4.44 ka, and 0.07 ka. Based on the age model, the ages of these boundaries are rounded to the nearest decade, but, of course, they are not this precise. Except for the date of European settlement (0.07 ka), which is based on the appearance of *Salsola* pollen, the 95% confidence ranges of the calibrated ^{14}C ages used for the age model are typically ~200 years (Grimm, 2011), which is the approximate error we would assign to these zone boundaries. Major cluster divisions occur at similar levels in the stratigraphically constrained analyses for both minerals and pollen. In the unconstrained analysis, we define 12 clusters, labeled 1–12 (Fig. S1). Although this analysis was not stratigraphically constrained, the samples from these clusters nevertheless show clear stratigraphic partitioning.

Clusters 1–4 characterize late Holocene zone E; whereas clusters 7–10 characterize mid-Holocene zone D (Fig. 8). Although a few samples from clusters 1–4 occur in the mid-Holocene and a few cluster 7-10 samples occur in the late Holocene, the clusters are predominantly either late or mid-Holocene. The zone D/E boundary sharply defines the break between the mid- and late Holocene clusters. With a stratigraphically constrained cluster analysis, a sharp change in the stratigraphic variables analyzed will tend to force a major division in the dendrogram, thus defining a zone boundary. However, samples on opposite sides of this zone boundary may be quite similar to each other. The unconstrained analysis, in which any sample or cluster can merge with any other sample or cluster, shows that the zone D samples are, in fact, quite distinct from the zone E samples. These two sets of four clusters (10–7, 4–1) each form a sequence of high to low aragonite values (Fig. 7). Thus, based on the aragonite proxy for moisture balance, each set of four clusters represents a wet to dry sequence. Wet-dry clusters alternate throughout the stratigraphic sequence (Fig. 8); however, the wet-dry phases of the mid-Holocene (zone D) are distinctive from the wet-dry phases of the late Holocene (zone E).

The mid-Holocene exhibits greater variability than the late Holocene (Fig. 8). Maximum aragonite values are similar in zones D and E; however, minimum aragonite values are less in the mid-Holocene. The pollen taxa further distinguish the mid-Holocene clusters 7–10 from the late Holocene clusters 1–4. All mid-Holocene clusters (7–10) have higher *Ambrosia*, higher Amaranthaceae, and lower *Artemisia* mean values than all late Holocene clusters (1–4). Thus, the mid-Holocene clusters are distinguished by high values of weedy taxa. In contrast to minerals and pollen, charcoal shows greater variability during the late Holocene, when presumably greater moisture during wet phases led to greater continuous fuel loads than available during the mid-Holocene (Brown et al., 2005).

Cluster 5, which groups with the late Holocene clusters in the dendrogram (Fig. S1) has values of aragonite, quartz, *Ambrosia*, and Amaranthaceae intermediate between clusters 1–4 and 7–10.

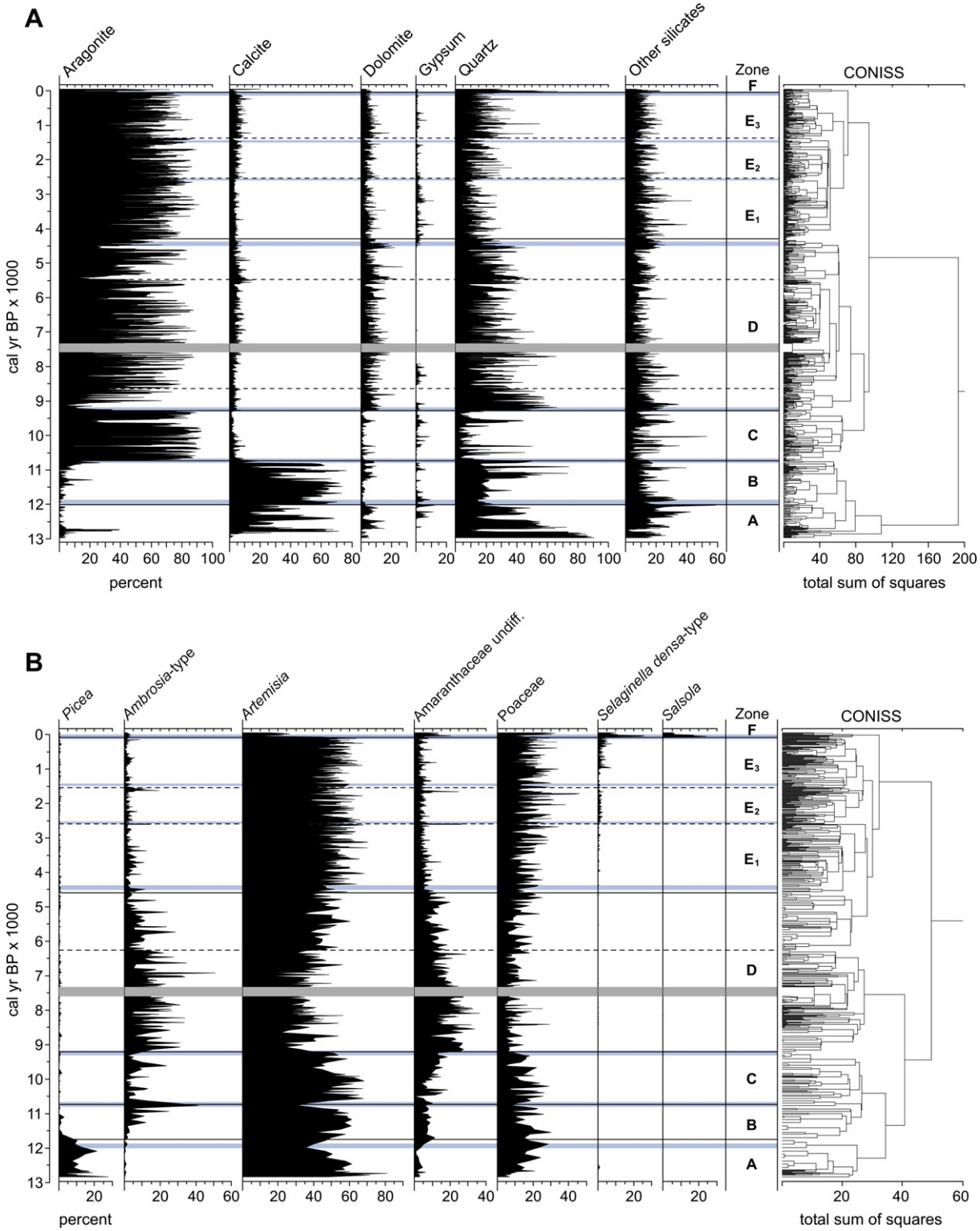

Fig. 6. Stratigraphic diagram for minerals (top) and pollen (bottom), with CONISS dendrograms and zones based on CONISS stratigraphically constrained cluster analysis. Solid black lines indicate primary divisions in the dendrogram. Dashed lines indicate secondary divisions. Blue bars indicate zones based on both dendrograms. The gray bar indicates the hiatus associated with the big slump.

However, it has high *Artemisia* values similar to late Holocene clusters 1–4, and it is most similar to the "driest" late Holocene cluster 4. Thus, cluster 5 is intermediate between the typical mid- and late Holocene assemblages, and it occurs in the upper part of zone D and the lower part of zone E.

Samples from cluster 1, the wettest late Holocene cluster, based on high aragonite and Poaceae, also dominate early Holocene zone C. Cluster 11 is mainly confined to the Pleistocene/Holocene transitional zone B (Fig. S1), and cluster 12 characterizes the late Pleistocene *Picea* zone A.

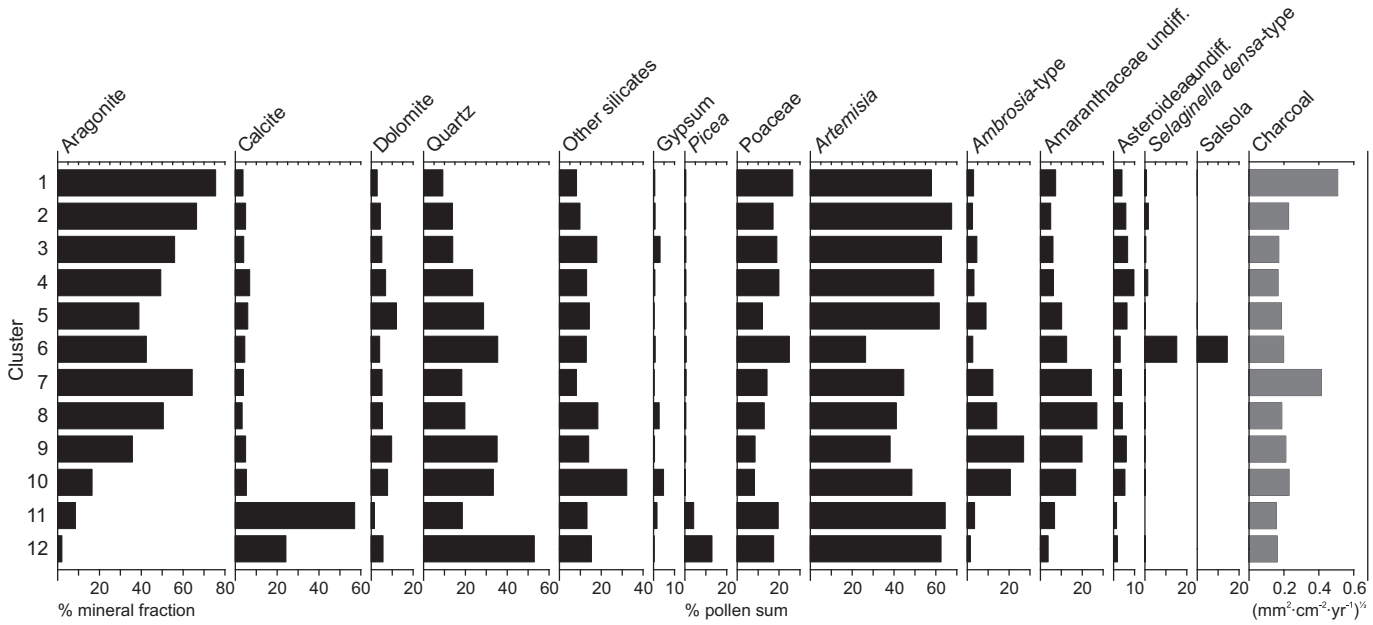

Fig. 7. Cluster mean values for minerals, pollen, and charcoal.

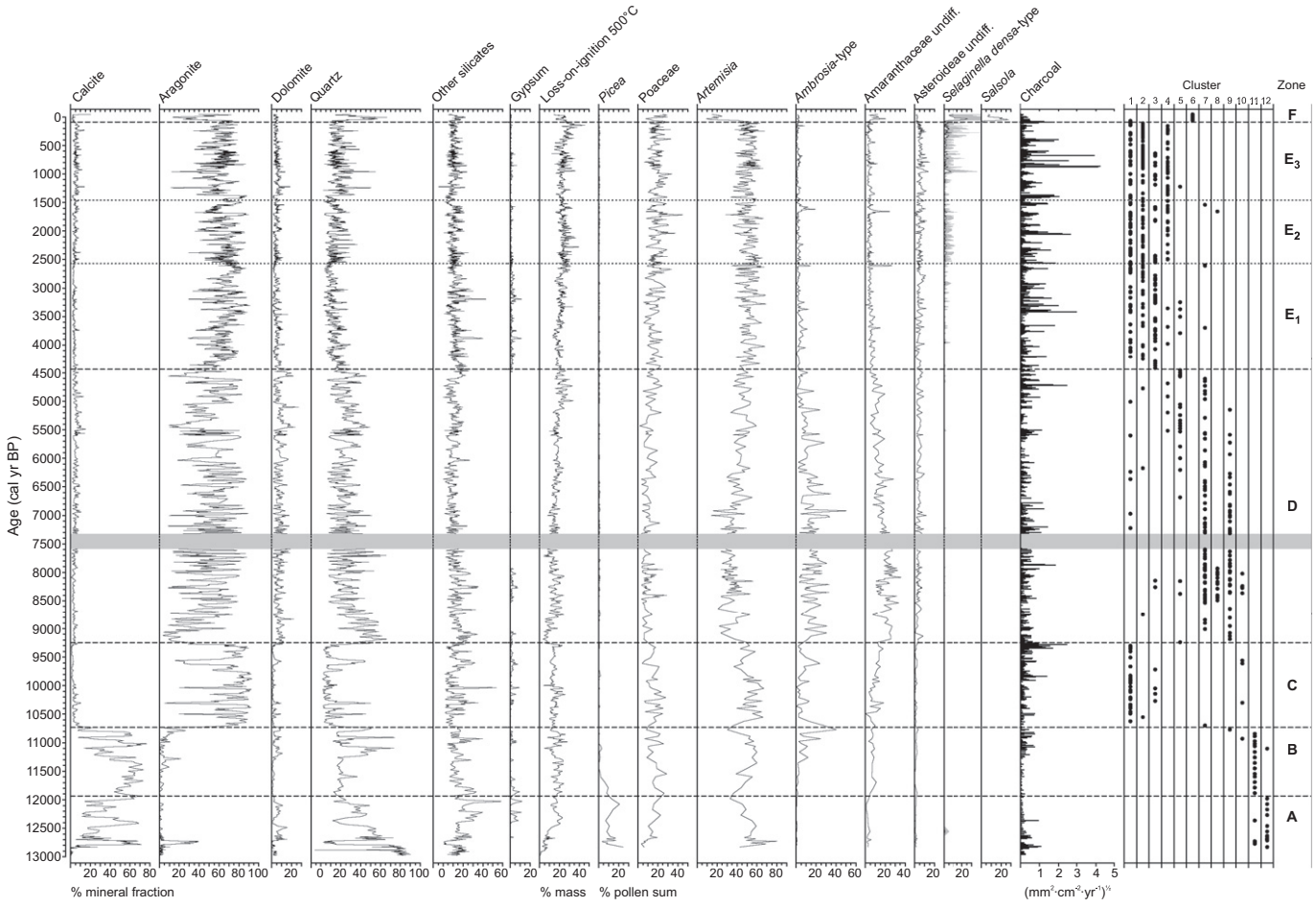

Fig. 8. Stratigraphic diagram of minerals, pollen, and charcoal. Dashed and dotted lines show zone and subzone boundaries based on CONISS stratigraphically constrained cluster analysis. Columns of dots on the right side of the diagram show the stratigraphic distributions of samples falling into clusters defined by the stratigraphically unconstrained CONISS cluster analysis (Fig. S1). The gray bar indicates the hiatus associated with the big slump.

Cluster 6 is comprised of the post-European settlement samples, distinguished by high values of the introduced weed *Salsola* and high values of *S. densa*. Probably because if high values of quartz, related to human disturbance, cluster 6 groups as an outlying cluster with the mid-Holocene clusters 7–10 (Fig. S1).

PCA analysis amplifies the relationships seen in the cluster analysis. In the mid-Holocene (zone D), the variable loadings show three distinct groups in the first three dimensions (Fig. 9). Axis 1 separates a group dominated by aragonite, Poaceae, and charcoal (group D1), from two groups separated on axes 2 and 3: group D2 dominated by quartz, calcite, dolomite, *Ambrosia*, and Asteroideae; and group D3 dominated by gypsum and other silicates. The clusters defined in the unconstrained cluster analysis (Fig. S1) are separated by their sample scores in the PCA analysis (Fig. 9), and the spatial relationships in the variable and sample ordinations show the dominant variables in the clusters. The spatial relationships in the variable and sample ordinations are: group D1 and cluster 7, Amaranthaceae and cluster 8, *Artemisia* and cluster 5, group D2 and cluster 9, and group D3 and cluster 10. The variable means for cluster 10 (Fig. 7) show that high gypsum and other silicates (group F) are associated with intermediate values (for zone D) of the all the main pollen types.

For the late Holocene (Fig. 10), axis 1 separates group E1 dominated by aragonite, Poaceae, and charcoal, from a two groups separated on axes 2 and 3: group E2 dominated by quartz, calcite, dolomite, *S. densa*, and Asteroideae and group E3 dominated by gypsum, other silicates, *Ambrosia*, and Amaranthaceae. *Artemisia* has low loadings on the first two axes, lying amidst the three groups, and has a high loading on axis 3, separating it from the other groups. The spatial relationships in the variable and sample ordinations are: group E1 and cluster 1, *Artemisia* and cluster 2, group E2 and cluster 4, and group E3 and cluster 3.

Relationships are similar in the mid- and late Holocene, but with some differences. Groups D1 and E1 are comprised of the same three variables: aragonite, Poaceae, and charcoal, which covary throughout the Holocene and are the proxies for the wettest conditions. Groups D2 and E2 contain quartz, dolomite, calcite, and Asteroideae, which covary throughout the Holocene. These variables are the proxies for the driest conditions. *Ambrosia* is a member of groups D2 and E3, thus behaves somewhat differently in the mid- vs. late Holocene. Amaranthaceae behaves independently in the mid-Holocene, but in the late Holocene is a member of group E3 and is associated with *Ambrosia*. Group E2 member *S. densa* rarely occurs in zone D, has low loadings on all axes of the zone D ordination, and is not a member of group D2.

7.2. Mineral, pollen, and charcoal stratigraphy

7.2.1. Late Pleistocene zone A, 12.97–11.93 ka

The estimated age for the base of the core is 12.97 ka, which corresponds closely, albeit perhaps coincidentally, with the beginning of the Younger Dryas (YD) interval at 12.846 ± 0.138 ka (Lowe et al., 2008). Much of the sediment within zone A is sand, which may have originated from repeated collapses of the Kettle Lake basin as buried ice melted or as oversteepened slopes collapsed; if so, this high quartz content may be the result of lake-basin sedimentation-processes rather than climate. Zone A is the late Pleistocene *Picea* zone, with values of *Picea* just over 20%. Pollen from other trees and shrubs occurs only sparingly, except for *Salix* (5–10%) and *Shepherdia canadensis* (to 5%). Other arboreal taxa characteristic of the late-glacial period farther east, such a *Betula* and *Alnus*, occur in percentages no greater than background long-distance-transport values during the Holocene. A pistillate

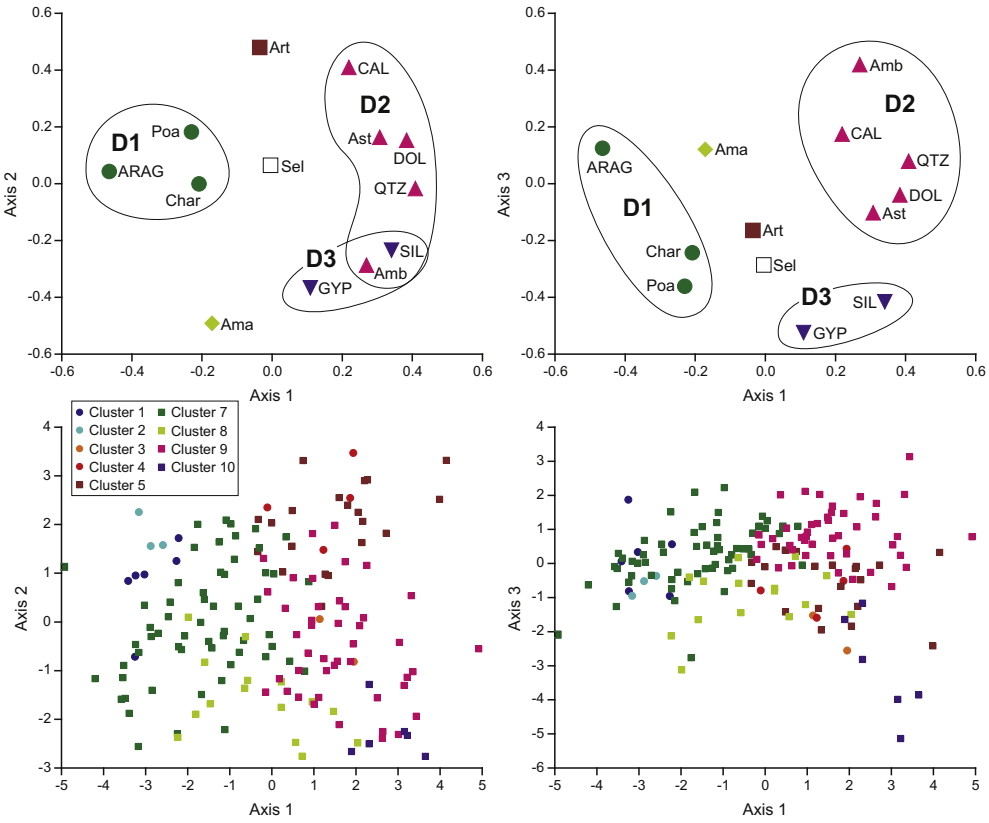

Fig. 9. Top: PCA loadings for major mineral, pollen, and charcoal variables in zone D. Bubbles labeled D1-D3 enclose variables associated on the first three axes. Bottom: PCA sample scores for zone D. Colors designate clusters defined in the stratigraphically unconstrained cluster analysis (Fig. S1).

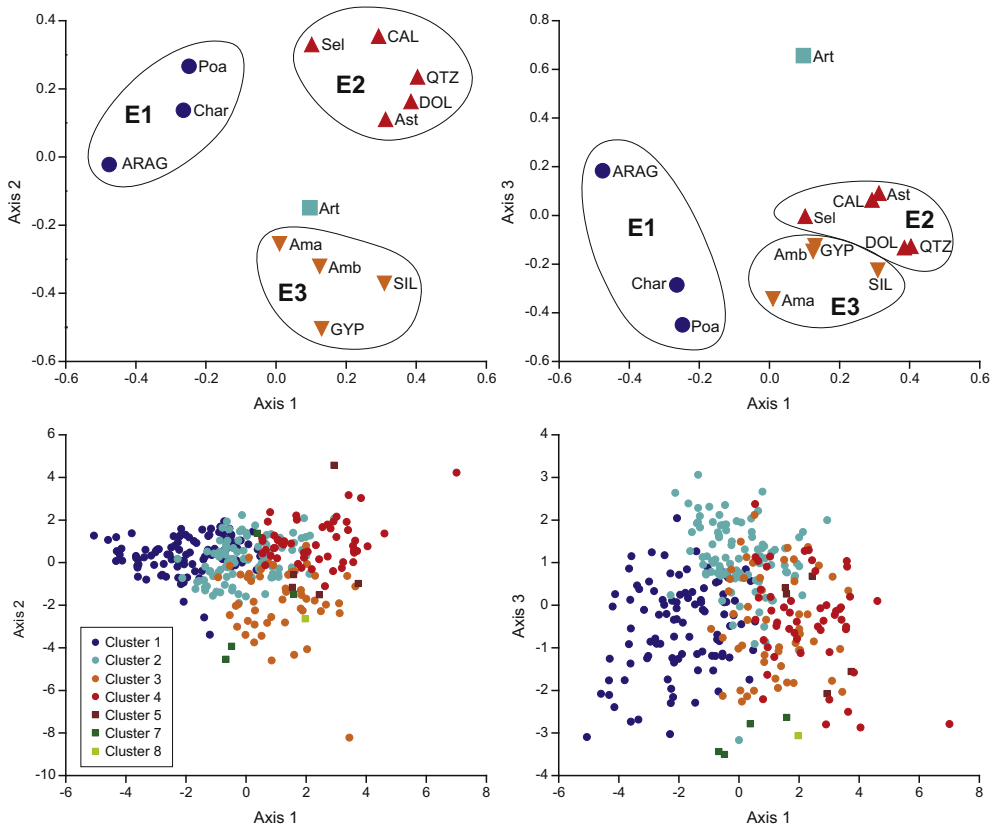

Fig. 10. Top: PCA loadings for major mineral, pollen, and charcoal variables in zone E. Bubbles labeled E1-E3 enclose variables associated on the first three axes. Bottom: PCA sample scores for zone E. Colors designate clusters defined in the stratigraphically unconstrained cluster analysis (Fig. S1).

catkin of *Alnus* at 2989–2990 cm depth confirms its presence at Kettle Lake; but this specimen, which is visible on the core image (Fig. 4B), was found in a slide or turbidite unit that produced two anachronic ^{14}C ages (Fig. 5). Thus, the confirmed presence of *Alnus* at Kettle Lake may pre-date our record (the specimen was not dated). *Pinus* percentages of <10% are less than Holocene values derived from long-distance transport. Quartz and calcite dominate the mineral suite, except for a spike of aragonite at 12.75 ka, visible in the core as a prominent white band at 3139–3154 cm depth (Fig. 3). Within Zone A, charcoal flux ranges 0–1.30 $(mm^2 \cdot cm^{-2} \cdot yr^{-1})^{½}$. However, a notable change in flux is evident at 12.37 ka as values abruptly decrease from a mean of 0.22 to 0.08 $(mm^2 \cdot cm^{-2} \cdot yr^{-1})^{½}$. Other than *Picea*, the dominant pollen types are the grassland taxa *Artemisia* and Poaceae, which are more abundant than *Picea*. These pollen spectra imply very open spruce parkland. The *Picea* pollen percentages are significantly lower than sites in eastern North Dakota, such as Moon Lake where *Picea* exceeds 60% during this time interval (Laird et al., 1998b), as well as NGP sites to the north, such as Hafichuk in Saskatchewan, where late-glacial *Picea* approaches 60% (Yansa, 2006).

7.2.2. Pleistocene/Holocene transition zone B, 11.93–10.73 ka

The zone A/B boundary is placed at 11.93 ka, which falls between major partitions in the mineral dendrogram at 12.02 ka and in the pollen dendrogram at 11.74 ka. The partition in the pollen dendrogram at 11.74 ka closely correlates with the end of the YD at 11.653 ka (Lowe et al., 2008). The final decline of *Picea* from 9% at 11.79 ka to <2% at 11.60 ka brackets the end of the YD. The pattern of charcoal deposition is comparable with the gradual decline in *Picea*, whereby higher flux values correspond with higher *Picea* percentage values, implying either greater incidence of fire or higher fuel loads. Pollen from other trees and shrub taxa occur at only low values; however, *Shepherdia argentea* characterizes this zone with values of 3–4%. Today, this characteristic NGP shrub occurs in protected draws and ravines; its greater abundance in zone B would indicate somewhat moister conditions than later in the Holocene. The appearance of *Ulmus* at values of 3–4%, which is higher than Holocene values, probably indicates local presence, and also somewhat moister conditions than present. The mineralogy changes from quartz to calcite dominance at the dendrogram partition at 12.02 ka.

Zone B is high in calcite, quartz, *Artemisia*, and Poaceae, with the lowest values of charcoal flux in the core, followed by an increase near the top of the zone. At ~11.3 ka, calcite and quartz begin to cycle back and forth, and this cycling between quartz and the dominant $CaCO_3$ mineral phase continues throughout the Holocene. High calcite and low quartz values in the early part of the zone from 11.9 to 11.3 ka imply relatively wet conditions. However, during this wet interval, *Picea* decreased and eventually disappeared as *Artemisia* and Poaceae dominate the pollen spectra, indicating the development of grassland. Therefore, the pollen data suggest that spruce parkland yielded to grassland under relatively moist conditions. Furthermore, low charcoal flux suggests that fire was infrequent during this time even though fuel-dense grasses were abundant. Therefore, an increase in temperature rather than a decrease in precipitation seems the more likely cause for the demise of *Picea*.

7.2.3. Early Holocene zone C, 10.73–9.25 ka

The zone B/C boundary is placed at 10.73 ka, which is the mean age of two similar partitions, one in the mineral dendrogram at

10.726 ka and the other in the pollen dendrogram at 10.735 ka. This boundary is marked by an abrupt switch from calcite to aragonite as the endogenic carbonate phase. Transition from calcite to aragonite depends on a threshold Mg:Ca ratio in salinizing lake water (Folk, 1974; De Choudens-Sánchez and González, 2009). Both phases cannot be precipitated concurrently. Aragonite increases to ~20% before the transition (Figs. 4 and 8), before the decline in all carbonates at the zone B/C boundary. The mixture of both aragonite and calcite in these transitional 1-cm sediment samples may represent interannual or seasonal fluctuations in the dominant endogenic phase as water chemistry was very near the Mg/Ca threshold.

The switch from calcite to aragonite deposition could result from either a sudden or gradual change in water chemistry. However, a hiatus in carbonate deposition occurs at the switch. Calcite drops at 2932 cm in the core, and aragonite then rises at 2928 cm (Fig. 4). A large spike of *Ambrosia* pollen and low charcoal flux coincide with this hiatus. Thus, zone C was initiated by a major drought, after which only aragonite precipitated.

The sediment of zone C is the most $CaCO_3$ rich in the entire core, with the least amount of quartz, suggesting considerable inflow of calcium-rich groundwater and generally moist conditions. However, deposition of aragonite rather than calcite suggests a higher Mg:Ca ratio than in zone B caused by higher evaporation (Shapley et al., 2010). The high rate of aragonite deposition suggests a climate with abundant winter precipitation favoring groundwater recharge and warm, dry summers promoting evaporation. This climate regime is consistent with the summer insolation maximum at 10.7 ka (e.g. COHMAP Members, 1988) and with the observed abundant *Artemisia*, which is common in regions with a winter precipitation-maximum (Williams et al., 2006).

Artemisia and *Poaceae* dominate the pollen spectra. Charcoal flux fluctuates and gradually increases throughout zone C, with consistently high values at the top of the zone at 9.35–9.25 ka. Samples from cluster 1 dominate zone C, but they do not strongly cycle with samples from other clusters as they do in late Holocene zone E. However, several low-aragonite/high-quartz episodes punctuate zone C at 100–500 yr intervals, indicating severe but relatively brief droughts during an otherwise humid interval. These droughts are indicated by samples in cluster 3, which represent late Holocene droughts, and cluster 10, which is a high-gypsum cluster that otherwise occurs in mid-Holocene zone D.

7.2.4. Middle Holocene zone D, 9.25–4.44 ka

The zone C/D boundary, separating the early and middle Holocene, is placed at 9.245 ka, which is the mean between major dendrogram partitions at 9.28 ka for minerals and 9.21 ka for pollen. Zone D was initiated by long, intense "megadrought" lasting ~200 yr, from 9.25 to 9.04 ka. This drought marks the beginning of the mid-Holocene interval, which is marked by low aragonite, *Artemisia*, and Poaceae and high quartz, *Ambrosia*, and Amaranthaceae (Fig. 11). The samples from this low-aragonite interval form a distinct cluster in the mineral dendrogram (Fig. 6).

This "megadrought" interval is bracketed by two slump units. Immediately below this section is a thick slump unit from 2780 to 2717 cm depth, which is a mixture of lithologies and which has a steeply dipping unconformable unit of laminated sediments at the base (Fig. 4). Above the low aragonite interval is a sandy unit, perhaps a turbidite rather than a slump, from 2700 to 2686 cm depth. Capping both of these units are several cm of fine-grained unlaminated sediment that may represent a plume that settled out of the water after the slump event. Bracketing the lower slump unit are two ^{14}C dates (Fig. 4), 8280 ± 40 ^{14}Cyr BP (CAMS-105790) at 2716 cm depth and 8305 ± 40 ^{14}C yr BP (CAMS-105791) with overlapping calibrated 95% age ranges of 9391–9128 cal yr BP and 9457–9249 cal yr BP respectively (Grimm, 2011), indicating very little sediment loss associated with this slump. Between these two slump units is finely laminated lake sediment. The low aragonite and low calcite character of this unit, unlike any earlier lake sediments, together with a pollen assemblage with high Amaranthaceae, dissimilar to any earlier, exclude the possibility that this section is slumped lake sediment. The slump or turbidite units suggest a rapid draw down of lake level and failure of sediments higher in the basin. Following a high aragonite, wet interval at 9.0 ka, three severe droughts occur in succession during the next 200 yr (Fig. 11), and these are terminated by another slump unit at 2669–2657 cm depth (Fig. 4). Thus, based on the aragonite proxy, generally very dry conditions prevailed from 9.25 to 8.8 ka, which represents the driest interval of the Holocene. The high Amaranthaceae values during this interval are consistent with this interpretation.

Clusters 7 and 9 occur throughout zone D, whereas clusters 8 and 10, characterized by high gypsum, occur early in the zone, ~8.5–7.9 ka. The cluster occurrences show a cyclic behavior as samples higher in aragonite, Poaceae, and Amaranthaceae alternate with clusters higher in quartz and *Ambrosia* (Fig. 7) at ~80–100 yr intervals. The variability in aragonite and quartz appear as lighter and darker bands in the sediment (Fig. 4). Charcoal-flux values fluctuate throughout the zone, oscillating between contiguous series of samples containing charcoal and samples having little or no charcoal.

In the PCA ordination (Fig. 9), Poaceae and charcoal group with aragonite; whereas *Ambrosia* groups with quartz. Cluster 7 has the highest charcoal and Poaceae and lowest *Ambrosia* of the mid-Holocene clusters. *Ambrosia* reaches values of 30% or more during the high quartz phases and groups with quartz in the PCA ordination (Fig. 9) and cluster analysis (Fig. 7). *Ambrosia* also reaches much higher values during the dry mid-Holocene than during the wetter late Holocene. *Artemisia* is independent of the aragonite-quartz mineralogy in both the cluster analysis and PCA ordination. Amaranthaceae are also independent aragonite-quartz in the ordination, but Amaranthaceae and *Artemisia* define the opposite ends of axis 2 in the ordination, although in the cluster analysis (Fig. 7) Amaranthaceae is higher in the high aragonite clusters. The association of aragonite with Poaceae and charcoal indicates wetter conditions favoring grass and producing higher fuel loads for fire (Clark et al., 2002; Brown et al., 2005). These wetter intervals alternated with droughts indicated by low aragonite and high quartz with an abundance of the weedy taxa *Ambrosia* and Amaranthaceae. A great diversity of herbaceous grassland pollen types characterizes Holocene zones D and E, although most taxa are scattered and occur at low abundances. Higher values of *Dalea*, *Eriogonum*, and Apiaceae, which includes ubiquitous dry-plains taxa such as *Musineon*, *Cymopterus*, and *Lomatium*, especially characterize zone D. Other typical NGP taxa characterizing zones D and E include *Allium*, *Sphaeralcea*, *Gaura*, and *Phlox*.

Asteroideae covaries with quartz in the PCA ordination (Fig. 9) and are more abundant in "dry" clusters 9 and 10. Although the Asteroideae are prominent members of the prairie vegetation, a number of Asteroideae expanded greatly during the 1930s drought, including *Erigeron strigosus*, *Conyza canadensis*, *Aster ericoides*, and *Solidago missouriensis*, at the expense of grasses. Weaver and Albertson (1936) wrote that in 1935 "So abundant were the weeds, that the prairies often appeared more like abandoned fields than grassland." These particular Asteroideae species are tall and many flowered, which may also explain the increase in Asteroideae pollen during drought intervals.

Most of the cluster 5 samples occur during two severe and lengthy droughts in the younger part of zone D, one at ~5.45–5.40 ka and the other at ~4.55–4.50 ka. The first of these is

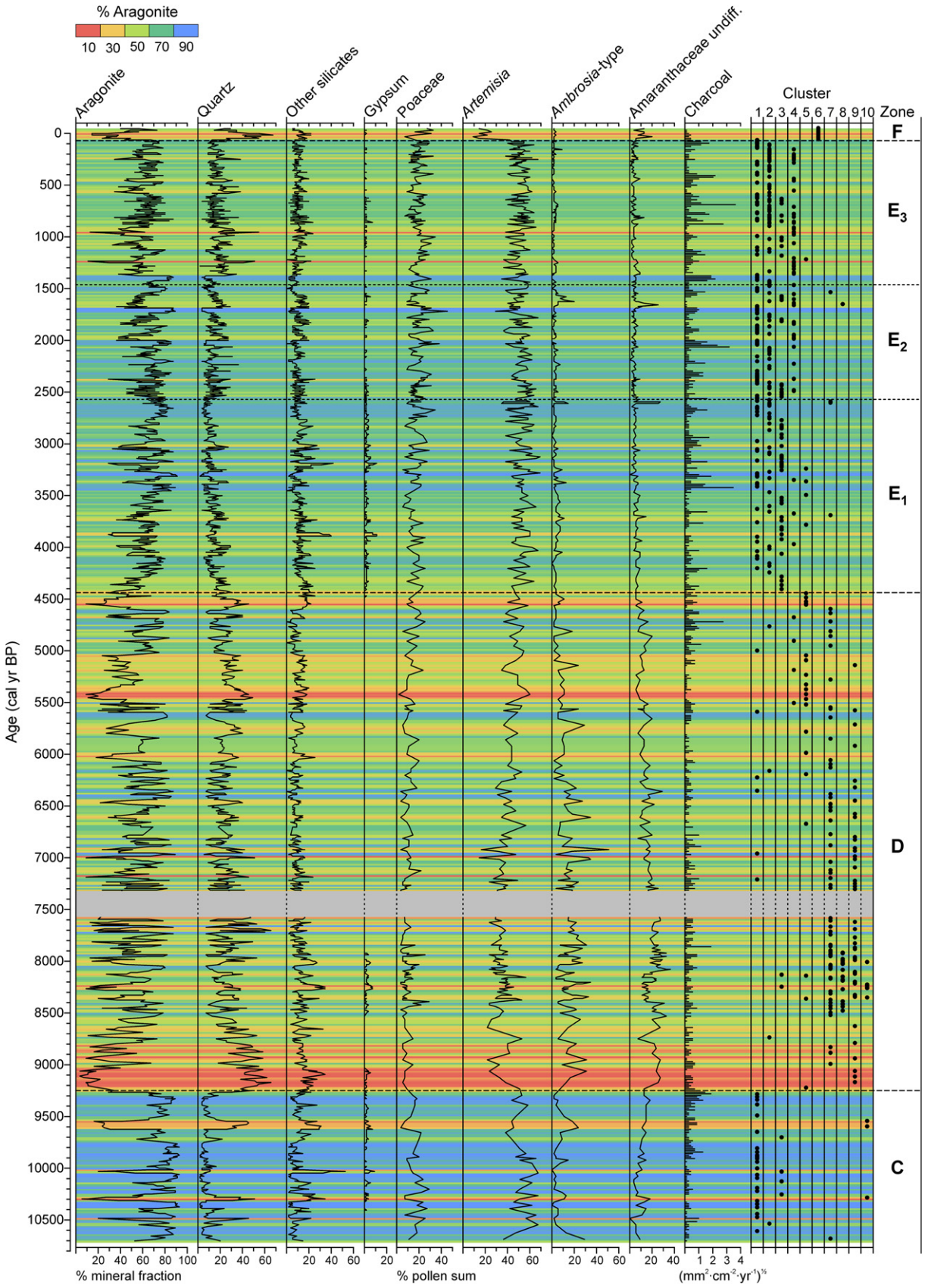

Fig. 11. Stratigraphic diagram of mineral, pollen, and charcoal variables with colors keyed to aragonite percentages. Presumed proxy interpretation is blue = wet and red = dry. Columns of dots on the right side of the diagram show the stratigraphic distributions of samples falling into clusters defined by the stratigraphically unconstrained CONISS cluster analysis (Fig. S1). The gray bar indicates the hiatus associated with the big slump.

the most severe drought of mid-Holocene after 9.0 ka. These multi-decadal drought episodes represented by cluster 5 may have been characterized by extended summer drought, unfavorable for weedy Amaranthaceae and *Ambrosia*, but with sufficient winter precipitation to support *Artemisia*.

Throughout the mid-Holocene, high quartz values imply that conditions were markedly drier compared to the early and late Holocene. However, high amplitude oscillations in minerals, pollen, and charcoal imply marked variability in moisture balance (Clark et al., 2002; Brown et al., 2005). During the wet phases, grassland expansion fostered high fuel loads, which in turn facilitated an increase in fire disturbance. In contrast, during the dry phases, decreased and discontinuous vegetation cover reduced burning.

The mineral and pollen data exhibit a strong cyclic pattern from 9.0 ka to 6.25 ka, when a major split occurs in the pollen dendrogram (Fig. 6). The cluster of pollen samples from 6.25 to 4.44 ka actually groups with the late Holocene, whereas the mineral samples from this section group with the mid-Holocene samples. Thus, the period from 6.25 ka to 4.44 ka is transitional between the mid- and late Holocene The dominant wet-dry cycles appear to have longer periods from 6.25 to 5.0 ka, after which strong century-scale cyclicity is again evident (Figs. 8 and 11). The most intense wet phase of zone D occurs at 5.2–5.1 ka, followed by the most intense drought since 9.0 ka at 5.45–5.40 ka. This drought is followed by a long period of intermediate aragonite values, indicating dry but not intensely dry conditions for the next several centuries until 5.05 ka. During the latter part of zone D after 6.25 ka, *Artemisia* increased gradually; and *Ambrosia*, although still highly variable, averaged less and peaks were not as great as during the previous three millennia. In addition, Amaranthaceae average less and Poaceae higher than the earlier part of zone D.

7.2.5. Late Holocene zones E and F, 4.44 ka–present

The zone D/E boundary, separating the mid- and late Holocene, is placed at 4.44 ka, which is the mean age between major partitions at 4.29 ka and 4.59 ka in the minerals and pollen dendrograms respectively. A decline in Amaranthaceae marks the D/E zone boundary. The mean values of aragonite are higher and quartz lower than in zone D. Among detrital minerals, dolomite is higher in zone D, whereas gypsum is higher and continuously present in zone E. *Artemisia* and Poaceae are higher in zone E than zone D, whereas *Ambrosia* and Amaranthaceae are lower. *S. densa*, which is rarely present in sediments older than zone E, occurs throughout zone E. As in zone D, charcoal-flux values fluctuate throughout zone E, but attain higher values than in any of the other zones.

The dendrograms for both minerals and pollen have two major partitions at approximately the same time, dividing zone E into three subzones (Figs. 6 and 8). These divisions are at 2.57 ka (minerals: 2.54 ka, pollen: 2.60 ka) and 1.46 ka (minerals: 1.37 ka, pollen 1.55 ka). Quartz values are lowest in zone $E_1$and increase in zones E_2 and E_3, whereas aragonite decreases. Subzone E_3 is particularly characterized by high values of gypsum. Differences in the abundance of *S. densa* also distinguish the subzones, with sporadic occurrences in E_1, continuous occurrence in E_2, and higher values in E_3. Spikes in *Ambrosia* and Amaranthaceae occur near the subzone boundaries.

Similar to the middle Holocene clusters, zone E clusters exhibit a highly cyclical behavior, with samples high in aragonite and Poaceae alternating with samples higher in quartz and slightly higher in *Ambrosia* and Asteroideae. However, the variances of the fluctuations are considerably less in zone E than in zone D. Maximum aragonite values are similar to zone D, but minimum values are greater, rarely dipping below 30%, a value that aragonite frequently falls below in zone D. Based on the aragonite proxy, a number of very wet intervals occurred from ~3.45–1.4 ka, with an extended wet period at 2.75–2.60 ka. Optical ages from a silt section at Rattlesnake Buttes in southcentral North Dakota indicate a period of soil formation commencing sometime before ~2.81 ka (Mason et al., 2008). This age corresponds generally with the onset of extended wet conditions evident at Kettle Lake. At Jones Lake, Manitoba, along the northern fringe of the NGP, *Quercus* rises at ~2.45 ka, about the time of the E_1/E_2 boundary and just following 150 yr wet period terminating subzone E_2.

Zone E_3 (1460–70 cal yr BP) shows a tripartite division. The oldest division (1460–900 cal yr BP) is drier with two severe droughts at ~1250 and ~950 cal yr BP. This interval corresponds with the Medieval Climatic Anomaly. A wet period with little variance persisted from ~900–600 BP, after which climate cycled more strongly with more severe droughts than the preceding interval. Given the distances and accuracy of the age control, correlation with megadroughts evident in the archaeological and tree-ring records (e.g. Woodhouse and Overpeck, 1998) would be premature. However, the "megadroughts" evident in the last millennium of the Kettle Lake record are small compared to the mid-Holocene.

Zone F is the post-European settlement horizon, and is marked by the appearance of *Salsola*, increased Amaranthaceae, and values of *S. densa* to 25%, which is four times higher than in any pre-European spectra. Quartz dominates the minerals, and charcoal values decline throughout the zone. All zone F samples fall into cluster 6, which is unique to zone F.

8. Discussion

8.1. The aragonite proxy for moisture balance

Given appropriate climatic, hydrologic, and limnologic conditions for endogenic aragonite formation, the aragonite proxy for moister balance is appropriate for groundwater flow-through lakes with no surficial inflows or outflows. It may also be most appropriate for lakes in coarse, permeable materials, such as Kettle Lake and the Ovando Valley lakes studied by Shapley et al. (2005), all of which are in glacial outwash. The association of high aragonite with high Poaceae and charcoal at Kettle Lake supports the case of Shapley et al. (2005) for using endogenic aragonite as a proxy for the rate of groundwater inflow into the lake. By extension aragonite is a proxy for groundwater recharge flux and ultimately for precipitation. The aragonite cycles are more pronounced in the generally drier mid-Holocene than in the wetter late Holocene. Thus, aragonite is a sensitive proxy for variations in groundwater inflow throughout the Holocene, and especially so for the dry mid-Holocene.

The sensitivity of aragonite as a precipitation proxy during the mid-Holocene at Kettle Lake contrasts with the diatom-inferred salinity proxy at Moon Lake, North Dakota (Laird et al., 1996a), which lost sensitivity during the mid-Holocene when the lake became hypersaline. The aragonite proxy is independent of salinity (provided the Mg/Ca ratio is high) and responds directly to the flow rate of water into the lake, which is a direct measure of humidity rather than salinity, which is a proxy for humidity.

Aragonite is a proxy for moisture balance, which is precipitation minus evapotranspiration. Thus, cooler, drier conditions may produce a response similar to warmer, wetter conditions. Seasonality of precipitation may also be a factor, as in this region of overall negative moisture balance, winter precipitation (non-growing season) is more likely to reach the groundwater than summer precipitation, which is evapotranspired (Winter and Rosenberry, 1995). Although we have emphasized aragonite, it covaries mainly with quartz, which is allogenic. At Kettle Lake, the primary source of quartz is probably eolian, because the lake has no surficial

inlets or even ravines of note in the small catchment. Furthermore, the highly permeable outwash in which the lake lies would inhibit surficial runoff except during the most intense storms or snowmelt events. Quartz values are generally high during the mid-Holocene, when the Pick City loess was being deposited in North Dakota (Artz, 1995; Mason et al., 2008), indicating considerable eolian activity. Thus, endogenic aragonite production and allogenic quartz input are inversely related, with increased quartz during dry periods not simply being a function of decreased aragonite production, but also of increased eolian input; and the aragonite proxy is actually an aragonite-quartz proxy.

8.2. The gypsum signal

Gypsum is often associated with arid conditions and is a moderately common endogenic lacustrine mineral in the NGP. Modern saline or hypersaline NGP lakes forming gypsum include Waldsea Lake (Last et al., 2002), Oro Lake (Last and Vance, 2002), Freefight Lake (Last, 1993), Clearwater Lake (Last et al., 1998), and Little Manitou Lake (Sack and Last, 1994). Other lakes have formed gypsum during drier past intervals, including Moon Lake (Valero-Garcés et al., 1997) and Medicine Lake (Valero-Garcés and Kelts, 1995). In such lakes, gypsum is endogenic, precipitating directly from the water column (Bowler and Teller, 1986; Valero-Garcés and Kelts, 1995).

At Kettle Lake, gypsum is below the detection limit over much of the Holocene, but is continuously present in zone E, especially E_1, and also within the older parts of zone D, as well as intermittently throughout zones C, B and A. Higher concentrations of gypsum occur within clusters 3 (late Holocene), 8 (mid-Holocene, 8.0–8.5 ka), and 10 (scattered intervals in the early to mid-Holocene). Gypsum covaries with other silicates in zone D (mid-Holocene) and with other silicates, *Ambrosia*, and Amaranthaceae in zone E (late Holocene) (Figs. 9 and 10). Gypsum does not closely covary with the other detrital minerals quartz, dolomite, or calcite, which suggests that gypsum and the other detrital minerals have different sources.

Gypsum is unlikely to have formed endogenically at Kettle Lake because salinity was never high and Ca concentrations would have been low under Ca-limiting carbonate production. Therefore, gypsum must derive from an allogenic source, and nearby saline lakes where the mineral did form are the most likely sources, such as Green Lake, 1.8 km NNE of Kettle Lake (Fig. 3), and Alkali Lake, 5.6 km E. Modern TDS in these lakes is in excess of 50,000 mg/L (Donovan and Grimm, 2007) but is highly variable over time based on antecedent precipitation, as the lakes are very shallow playas. Presumably, these lakes are saline because of a differing chemistry of groundwater inflow compared to Kettle or because of restriction in the amount of lake water leaving via groundwater outflow. In particular, based on location, outflow from Green Lake would be considered a candidate to flow into Kettle, but its saline water evidently does not enter modern Kettle through the subsurface.

To provide an eolian source of gypsum, a basin must hold water periodically in order for it to form, but must also dry out periodically to be subject to wind deflation. Such wet-dry cycling could occur either seasonally or at some multi-year or multi-decadal scale. During the mid-Holocene, the shallow lake basins currently producing gypsum were probably permanently dry (Donovan and Grimm, 2007), and would not have provided a constant source of gypsum. However, during generally wetter conditions of the late Holocene, these lakes probably did periodically hold water during wet seasons or years, drying out seasonally or during dry years. Other salts besides gypsum, e.g., Na-Mg-SO4 salts; (Last, 1984), would also have formed, but these salts are much more soluble than gypsum and may not have been preserved.

The detrital minerals quartz, calcite, and dolomite are associated with low-aragonite/high-Poaceae dry phases, which suggests that their eolian sources are areas denuded of vegetation during extreme drought. In contrast, the sources for gypsum are playa lake beds periodically exposed during wetter periods. In the late Holocene, gypsum is associated with Amaranthaceae (Fig. 10), and in the mid-Holocene, gypsum is associated with cluster 8, which has the highest average value of Amaranthaceae (Fig. 7). A number of Amaranthaceae species colonize alkaline or saline lake beds, e.g. *Atriplex subspicata*, *Chenopodium rubrum*, Monolepis nuttalliana, *Salicornia depressa* (Larson, 1993; Stubbendieck et al., 1995). Thus, the association of gypsum with Amaranthaceae indicates the aerial exposure of playa lake beds, which become an eolian source for both gypsum and Amaranthaceae pollen.

8.3. Younger Dryas aragonite peak and the "Clovis drought"

Although calcite dominates the $CaCO_3$ mineral phase in zone A (Fig. 8), which corresponds to the Younger Dryas interval, a pronounced yet isolated aragonite layer occurs in the early YD centered at 12.75 ka. This layer suggests that a relatively short dry episode occurred at that time. The decline in *Picea* and rise in *Artemisia* during this interval further implies an opening of the vegetation as spruce parkland yielded to *Artemisia*-dominated steppe. A concomitant decline in charcoal suggests an overall reduction in fuel availability and less fire disturbance.

Recent work from northern Illinois (Gonzales and Grimm, 2009; Gonzales et al., 2009) indicates that the warmest interval of late-glacial time occurred during the late Allerød and early YD (~13.2–12.5 ka), with a short interval of reduced precipitation in the early Younger Dryas, followed by cooler, wetter conditions (Gonzales et al., 2009). The early YD aragonite interval at Kettle Lake is therefore coeval with a short warm-dry interval in this accurately-dated record from northern Illinois and also corresponds with the Clovis cultural period of ~11.05–10.8 ^{14}C yr BP (Waters and Stafford, 2007), which calibrates to ~13.1–12.6 cal yr ka. Haynes (1991, 2008) has argued for a "Clovis drought" followed by wetter conditions during the YD based on evidence from sites widely distributed from California to Missouri and Arizona to South Dakota. Holliday (2000) contended that the Clovis period on the southern High Plains was wetter than the succeeding Folsom cultural period and that evidence for a major drought is lacking. In contrast, recent soil δ^{13}C evidence from southwest Missouri on the eastern margin of the central Great Plains shows an expansion of C_4 grassland and inferred aridity during the YD (Dorale et al., 2010). Thus, evidence for YD moisture trends in the mid-continent is inconclusive and may vary regionally. The Clovis-age aragonite layer from Kettle Lake, coupled with the *Picea*, *Artemisia* and charcoal records, is consistent with the hypothesis for a "Clovis drought" in the NGP, albeit brief.

8.4. Early Holocene droughts and Lake Agassiz

Northeast of Kettle Lake by ~360 km at its nearest, Lake Agassiz first formed ~13.67 ka when ice retreated north from the Big Stone Moraine near the continental divide between the south-flowing Minnesota River and the north-flowing Red River (Lepper et al., 2007). Lake Agassiz may have influenced early Holocene NGP climate. Mesoscale climate modeling by (Hostetler et al., 2000) indicates enhanced precipitation in the NGP associated with a large Lake Agassiz at 11 ka. This result is consistent with inferred humid conditions at Kettle Lake during zone C time, as evidenced by high values of carbonate (Fig. 8). However, zone C and the upper part of zone B were punctuated by several episodes of low carbonate (inferred drought) spaced at ~100–300 yr intervals. The early Holocene Nipigon phase of Lake Agassiz corresponds closely in time

with zone C, ~10.7–9.2 ka (Leverington et al., 2002). During this phase, the lake abandoned the southern outlet and overflowed into the Nipigon and Superior basins. However, the lake fluctuated in size, and high water levels are marked by strandlines, which mark maximum transgressions following rapid drainages of the lake as ice retreat opened new outlets. According to this model, a transgressive cycle was initiated by opening of a new outlet, with an abrupt drop in lake level, and gradual isostatic rebound causing transgression of the southern lake margin and beach construction. A preserved beach-strandline elevation then represents the maximum lake level and size achieved before a sudden drop caused by opening of a new outlet. (Leverington et al., 2002; Leverington and Teller, 2003; Teller and Leverington, 2004).

Teller and Leverington (2004) list nine strandlines between the Upper Campbell and Stonewall beaches. The number of inferred droughts in zone C at Kettle Lake is similar to the number of Lake Agassiz strandlines for the Nipigon phase. However, dating of the strandlines is not robust and disagreement exists over the ages of the strandlines below the Upper Campbell beach. Fenton et al. (1983) believed that some of these strandlines formed during earlier Moorhead phase, not Nipigon, and new radiocarbon and OSL dates indicate that one of these, the Ojata beach, is Moorhead in age (Fisher et al., 2008). Nevertheless, transgressing shorelines will tend to erode existing beaches they cross, and strandlines below the Upper Campbell beach should in general be younger than the Upper Campbell beach, i.e. Nipigon in age. In any case, uncertainty in the number and age of Nipigon strandlines is sufficiently large that "wiggle-match" correlations are not possible; however, the largest inferred droughts, which bracket zone C, are similar in sequence to the two largest Lake Agassiz outbursts during this period, with drops in lake level of 30 m post-Upper Campbell and 58 m post-Stonewall (Leverington and Teller, 2003; Teller and Leverington, 2004). Until these beaches are better dated, this speculated correlation between beaches in Lake Agassiz and droughts at Kettle Lake is a hypothesis to be tested. Further to be tested is the mechanism connecting droughts at Kettle Lake with Lake Agassiz draw downs. Possibilities include a lake-size effect as modeled by Hostetler et al. (2000) or effects of Agassiz outbursts on North Atlantic thermohaline circulation as suggested by Teller and Leverington (2004).

8.5. The 9.25 ka event

A major shift to drier climate at ~9.25 ka is evident in records from across the NGP. several of these sites have relatively few dates, many of which are on bulk sediment, so ages are approximate. At Clearwater Lake, southwestern Saskatchewan, a pedogenic layer formed at ~9.23 ka, when the lake completely dried out (Last et al., 1998). Chappice Lake, southeastern Alberta, also went dry sometime prior to ~8.1 ka (Vance et al., 1992, 1993). At Oro Lake, southern Saskatchewan, the driest, hypersaline conditions of the Holocene occurred from ~10.5–8.2 ka, with maximum salinity at ~9.3 ka (Last and Vance, 2002). At Devils Lake, northeastern North Dakota, salinity, inferred from diatoms (Fritz et al., 1991) and from the geochemistry of endogenic carbonate and fossil ostracodes (Haskell et al., 1996), reaches a maximum at ~8.9 ka, although the entire Holocene chronology is controlled by only four AMS radiocarbon dates. At Moon Lake, southeastern North Dakota, diatom-inferred salinity peaks at ~9 ka, but this age is approximate as it is bracketed by two ^{14}C ages separated in excess of 2 ka (Laird et al., 1998b). In northwest Minnesota, prairie taxa begin to expand at accurately-dated deep and Steel lakes at ~9.4 ka (Wright et al., 2004; Nelson and Hu, 2008). Williams et al. (2009) recently reviewed and updated the early Holocene history of prairie expansion on the eastern and northern borders of the NGP, and according to this analysis, the most rapid ecotone movement occurred between 10 and 9 ka. Finally, the younger age limit on the Leonard paleosol is ~9.3 ka (Artz, 1995; Haynes, 2008). The widespread organic-rich Leonard paleosol characterizes the late Pleistocene-early Holocene Aggie Brown member of the Oahe formation, which includes postglacial sediments in North Dakota (Clayton et al., 1976; Artz, 1995; Mason et al., 2008). Dates on the Leonard paleosol range from ~13.7–9.3 ka (11.86–8.3 ^{14}C ka) (Artz, 1995; Haynes, 2008). This soil is then buried by loess, which represents the Pick City member of the Oahe formation (Clayton et al., 1976; Artz, 1995; Mason et al., 2008). In the central Great Plains, the early Holocene Brady paleosol, which is correlative to the Leonard paleosol, is buried by the middle Holocene Bignell loess, which began accumulating 10–9 ka, based on OSL ages (Miao et al., 2005). Thus, a number of various proxies indicate a significant shift to drier climate between 10 and 9 ka. The dating on many of these records is too poor to narrow this range down precisely. The 9.25 event at Kettle Lake may accurately date the regional maximum of Holocene aridity across the NGP, although this hypothesis remains to be tested by dates of comparable quality from other sites.

The 9.25 ka drought correlates well with a δ^{18}O minimum in the Greenland ice cores, variously called the 9.3 ka (e.g. Shao et al., 2006; Vinther et al., 2006; Came et al., 2007; Marshall et al., 2007; Rasmussen et al., 2007; Yu et al., 2010) or 9.2 ka event (e.g. Fleitmann et al., 2008). This "9.25 ka event" is of similar magnitude to the perhaps better known 8.2 ka event (e.g. Alley and Ágústsdóttir, 2005; Rohling and Pälike, 2005), but of shorter duration. Rasmussen et al. (2007) indentify the 9.25 ka event by a δ^{18}O minimum at 9.245–9.225 ka (converted from the GICC05 b2K time scale) and by an ice-accumulation minimum at 9.27–9.23 ka. These intervals correspond closely with the zone C/D boundary at 9.245 ka. The 9.25 event is associated with cooling at high and middle latitudes and drying in the northern tropics and at sites across Europe, Middle East, Asia, Alaska, and Canadian Arctic (Shao et al., 2006; Came et al., 2007; Marshall et al., 2007; Fleitmann et al., 2008) and is associated with a meltwater pulse (Fleitmann et al., 2008).

The 9.25 ka event also corresponds with a major drawdown of ~58 m and northward retreat of Lake Agassiz following the Stonewall beach stage at ~9.2 ka, when Agassiz retreated far into Canada from North Dakota and became much reduced in area (Leverington et al., 2002; Teller et al., 2002; Teller and Leverington, 2004). Although the outburst of water from this event in terms of volume was not as great as that of the 8.2 ka event, the areal retreat is similar (Teller et al., 2002; Fleitmann et al., 2008), and importantly Agassiz withdrew into Canada far from Kettle Lake. The 9.25 ka event has also been associated with a 45-m drawdown of Lake Superior caused by the failure of a glacial drift dam (Yu et al., 2010), and possibly this event together with the Agassiz drawdown contributed to its global effect. Although, the Agassiz meltwater outburst from the 8.2 ka event was substantially larger and globally may have had a greater effect, the lake was much more distant from Kettle Lake at this time. Thus, the 9.25 Agassiz event may have had a greater impact in the NGP than the 8.2 ka event, which is not evident as a major event in the Kettle Lake data. With the rapid retreat of Lake Agassiz to the north at 9.25 ka, the climate of the NGP was suddenly thrust into an insolation controlled regime.

8.6. Mid-Holocene Amaranthaceae, Ambrosia, and high variability

The amplitudes of the oscillations in minerals, especially aragonite and quartz, and pollen, especially *Ambrosia* and Amaranthaceae, are much higher during the mid-Holocene (zone D) than during the early and late Holocene. This high variability suggests

great variability in precipitation. Although Amaranthaceae were more abundant during the dry mid-Holocene than during the early and late Holocene, within mid-Holocene zone D, Amaranthaceae are most abundant in clusters having the highest values of aragonite and Poaceae (Fig. 7), i.e. the "wet" clusters. However, in the PCA ordination (Fig. 9), Amaranthaceae are not closely associated with the "wet" aragonite-Poaceae-charcoal group. Amaranthaceae includes a number of weedy species that grow on uplands (e.g. *Amaranthus albus*, *Amaranthus retroflexus*, *Krascheninnikovia lanata*) as well as on mud flats (e.g. *Atriplex subspicata*, *Chenopodium rubrum*). Thus, different Amaranthaceae species may have characterized the wet vs. dry mid-Holocene phases. During wetter periods, the myriad of prairie potholes in the region may have seasonally held water, drying out during summer, exposing habitats ideal for mudflat Amaranthaceae. During dry phases, other weedy Amaranthaceae may have expanded in upland habitats. In addition, extremely drought resistant perennial Amaranthaceae such as the shrubby *Krascheninnikovia lanata* may have expanded during long-term drought. Thus, during the mid-Holocene Amaranthaceae were more abundant during both dry and wet phases compared to the late Holocene. The overall signal of abundant Amaranthaceae during the mid-Holocene is one of high variability favoring weedy species.

In general, high variability should favor the weedy *Ambrosia*. However, *Ambrosia* is not very drought tolerant, and the high abundance of *Ambrosia* during the dry mid-Holocene seems somewhat paradoxical (Grimm, 2001; Craine and McLauchlan, 2004). The possibility that *Ambrosia* was growing on exposed lake beds during drought is unlikely, because *Ambrosia* must germinate in spring before lake marginal areas are typically exposed as lakes draw down during summer (Grimm, 2001). *Ambrosia* seeds are rarely found as macrofossils in lake sediments, whereas various species of Amaranthaceae, especially *Chenopodium* species which colonize mud flats, are commonly found (e.g. Watts and Bright, 1968; Van Zant, 1979; Yansa, 1998, 2006; Yansa and Basinger, 1999; Yansa et al., 2007). *Iva axillaris*, which is included in *Ambrosia*-type, does grow on mudflats (Stubbendieck et al., 1995); however, its seeds have not been found as macrofossils, and only a few *Ambrosia* seeds have been found, and these are the upland *Ambrosia artemisiifolia* and *A. psilostachya* (Watts and Bright, 1968; Van Zant, 1979; Laird et al., 1996a).

Indeed, because of the drought intolerance of *Ambrosia* and observations that *Ambrosia* increases with grazing, Craine and McLauchlan (2004) suggested that grazing, especially by bison, is a more plausible explanation than drought for high abundance of *Ambrosia*. Nonetheless, *Ambrosia* is more abundant across the NGP during the drier mid-Holocene than during the wetter late Holocene (Grimm, 2001). Moreover, high values of *Ambrosia* correspond with low aragonite, high quartz, and low charcoal; thus, *Ambrosia* is most abundant during the driest phases of the mid-Holocene. We suggest that the key to this paradox is differing temporal scales of climatic variability. The wet-dry cycles at Kettle Lake during the mid-Holocene are multi-decadal, 80–100 years on average. Thus, on average, 40–50 years of drought alternated with 40–50 years of wetter conditions. However, the half-century droughts may not have been 40–50 years of continuous intense drought, but rather a series of severe decadal or sub-decadal droughts interspersed with wet years. Frequently recurring droughts that repeatedly disturbed the vegetation would have created favorable conditions for *Ambrosia* during alternating wet years. The high values of *Ambrosia* during long, generally dry periods strongly suggest that these dry periods must have been interspersed with wet summers. Thus, high interannual variability in precipitation during the multi-decadal dry phases may explain the abundance of the weedy, but drought intolerant, *Ambrosia* during the mid-Holocene. The grazing hypothesis for high *Ambrosia* is not supported as an alternative to the climatic hypothesis, because *Ambrosia* undeniably was more abundant during on-average drier periods. Moreover, *Ambrosia* was less abundant during the late Holocene, and large peaks of *Ambrosia* characteristic of the mid-Holocene are absent during the late Holocene, when large herds of bison roamed the NGP.

Seasonality of precipitation may also explain low lake levels and *Ambrosia*. Lake levels are particularly responsive to winter precipitation, because much of the summer precipitation is evapotranspired, whereas winter precipitation recharges groundwater (Winter and Rosenberry, 1995). A reduction of winter precipitation during the mid-Holocene would have removed the buffering effect of this precipitation on summer drought, inasmuch as winter precipitation recharges soil moisture available to plants during summer (Grimm, 2001). Thus, the vegetation would have been more sensitive to variations in summer precipitation. If mid-Holocene summer precipitation were highly variable as today, in the absence of drought-buffering winter precipitation, dry summers would have had a greater impact on vegetation, creating open areas favorable for *Ambrosia* during succeeding wet summers. A reduction of winter precipitation is also consistent with the decrease in *Artemisia* during the mid-Holocene. Today, *Artemisia* increases westward across the NGP with decreasing moisture, but *Artemisia* did not increase during the drier mid-Holocene at Kettle Lake or at other sites across the NGP (Grimm, 2001). Although *Artemisia* fluctuates during the mid-Holocene, these fluctuations do not align with either the driest or wettest phases.

In contrast to the high variability in pollen and minerals during the mid-Holocene, charcoal is more variable during the late Holocene. Higher charcoal fluxes imply more fuel or more fires owing to more fuel, and a higher fuel loads are consistent with wetter climate during the late Holocene.

8.7. The 4.44 ka event

Many sites across the NGP show a shift to wetter climate in the late Holocene. The exact timing varies with site and proxy. Brief episodes of soil formation were underway by 5.7–4.4 ka (Artz, 1995), and paleosols within the late Holocene Riverdale member of the Oahe formation indicate periods of landscape stability (Artz, 1995; Mason et al., 2008). The 4.44 ka mode shift at Kettle Lake is evident in both minerals and pollen. The stratigraphically constrained cluster analyses of both proxies have major breaks at this time (Fig. 6), and in the combined mineral-pollen cluster analysis, a clear break occurs at ~4.44 ka (Fig. 11). Nevertheless, after ~7 ka the primary pollen taxa show gradual trends—*Ambrosia* and Amaranthaceae decreasing, *Artemisia* increasing—and the mode shift at 4.44 ka is not as dramatic as that at 9.25 ka. In addition, a shift in pollen is evident at 6.25 ka. In the interval from 6.25 to 4.44 ka, pollen samples cluster with late Holocene samples, whereas mineral samples cluster with mid-Holocene samples (Fig. 6). Data from a newly published, well dated site along the northern margin of the NGP, Jones Lake, Manitoba (Teed et al., 2009) show a mid-Holocene zone with high *Ambrosia* beginning at ~ 9.1 ka, similar to the beginning of zone D at Kettle Lake. However, *Ambrosia* values fall to late Holocene levels at ~6.3 ka. Thus, at this time a quantitative shift in pollen occurred at Kettle Lake, but the climatic forcing was not great enough to cause a mode shift, whereas at Jones Lake along the prairie margin, it was.

Kettle Lake shows little evidence for an extraordinary "mega-drought" 4200 years ago as Booth et al. (2005) postulated as a continental phenomenon, with evidence of dune reactivation in the Great Plains. The shift at 4.44 ka at Kettle Lake is to generally wetter climate. High aragonite values and by proxy wet conditions occurred 4.2–4.1 ka. Conditions were somewhat drier in the

subsequent interval ~4.1–3.85 ka, although based on the combined mineral-pollen cluster analyses, this period was distinctly late Holocene in character, not mid-Holocene. Possibly, dunes did reactivate during this somewhat drier period, as they did several times during the late Holocene (Muhs et al., 1997; Wolfe et al., 2000; Forman et al., 2005; Miao et al., 2007). However, this drought event was not unusually intense; rather it was a short-lived episode that followed the sustained activity evident in the mid-Holocene (Forman et al., 2001; Wolfe et al., 2002).

8.8. Asymmetric response to mid-Holocene aridity

Several investigators have noted the "asymmetric" response of prairie vegetation to mid-Holocene aridity, with rapid prairie expansion during the early Holocene followed by gradual retreat during the late Holocene (Umbanhowar et al., 2006; Nelson and Hu, 2008; Williams et al., 2009). This behavior could be a response to asymmetric climate change (i.e. rapid early Holocene vs. gradual late Holocene climate change) or an asymmetric ecological response of vegetation to climate change, particularly as mediated by fire. Tree death, perhaps assisted by fire, may occur rapidly; whereas forest expansion may be impeded by prairie fires, especially as prairie fuel loads increase with increased precipitation (Umbanhowar et al., 2006). However, Nelson and Hu (2008) note that the sudden early Holocene shift of forest to mixed-grass prairie occurred without an intervening period of tallgrass prairie, whereas the late Holocene prairie to forest transition included a tallgrass prairie phase, which suggests asymmetric climate change. These studies have focused on sites along the prairie-forest border, rather than on sites within the NGP where prairie has persisted for the entire Holocene. Climatic interpretations from changes among prairie pollen taxa that record changes within the prairie vegetation are not confounded by the potential problem of ecological inertia involved with prairie-forest transitions (Grimm, 1987; Umbanhowar, 2004a; Umbanhowar et al., 2006). In addition, the synoptic mapping of the prairie-forest border and the observed asymmetric response considers only prairie vs. forest and does not chronicle changes within the herbaceous prairie pollen types, which are lumped together.

The Kettle Lake record provides a climatic explanation for the observed asymmetric response along the prairie-forest border. The shift from moist to arid conditions was abrupt at 9.25 ka with the onset of the most extreme drought of the Holocene, with potentially devastating effects on vegetation. On the other hand, the shift to wetter climate in the late Holocene was more gradual with mode shifts at different times at different places and with opportunity for transitional vegetation types to develop. The cause for the asymmetry may be response to orbital forcing and regional effects of the Laurentide ice sheet and Lake Agassiz. With the retreat of Lake-Agassiz far to the north ~9.25 ka, the climate of the NGP was suddenly thrust into an insolation controlled regime. Whereas in the late Holocene, climate was slowly changing as perihelion moved to winter.

8.9. Selaginella densa in the late Holocene

The occurrence of *S. densa* (prairie club-moss) characterizes late Holocene zone E, and quantitative differences distinguish subzones within zone E. *S. densa*, which forms cushion-like mats 1–2 cm in height, is very common in the northern mixed-grass prairie (Coupland, 1950; Lauenroth and Whitman, 1977; Hall-Beyer and Gwyn, 1996). It increases in abundance with grazing (Clarke et al., 1943; Hubbard, 1951; Taylor and Lacey, 1994), probably because it cannot compete for light with taller grasses and forbs (Smoliak, 1965). Even light grazing will cause it to increase in abundance (Smoliak, 1965), with rotational grazing facilitating a marked response (Clarke et al., 1943; Hubbard, 1951; Smoliak, 1960). *S. densa* shows a step-like increase in the subzones of zone E, and it increases to 25% in the post-European settlement zone F. Two hypotheses might explain its late Holocene appearance and increasing abundance. The first is climatic. The range of *S. densa* is the NGP and alpine meadows in the Rocky Mountains (Valdespino, 1993). It does not occur in the central and southern Plains. Thus, *S. densa* may have increased in the NGP during the late Holocene in response to cooler temperature. The species is extremely drought resistant (Webster and Steeves, 1964), thus increased precipitation—and increased grass cover—is an unlikely cause for its noted increase in abundance during the late Holocene. The second hypothesis is that *S. densa* increased in the late Holocene in response to increased grazing pressure from bison. The modern form of bison appeared in late Holocene ~5 ka, when populations expanded (McDonald, 1981). Thus, *S. densa* may a proxy for bison population size. Supporting this hypothesis is the greatly increased values of *S. densa* with European settlement and intense cattle grazing. The two hypotheses are not mutually exclusive.

8.10. Climate drivers

Precipitation variations in the NGP have been linked with tropical Pacific SSTs, with above (below)-normal precipitation associated with above (below)-normal SSTs. In addition, wetter (drier) summer conditions are associated with El Niño (La Niña) events (Bunkers et al., 1996; Ting and Wang, 1997; Schubert et al., 2004a; Seager et al., 2005; Wu and Kinter, 2009). Low Pacific SSTs combined with weak ENSO activity characterized the 1930s drought (Schubert et al., 2004a). Decadal-scale moisture variations are associated with the Pacific decadal oscillation and the North Pacific mode (Barlow et al., 2001; Castro et al., 2001). However, correlations with Pacific SSTs, although significant, are not very high, and Atlantic SSTs and the North Atlantic oscillation also appear to influence Great Plains precipitation, particularly as they influence the Bermuda high and moisture transport into the Great Plains, particularly during summer (Ruiz-Barradas and Nigam, 2005; Schubert et al., 2008; Weaver and Nigam, 2008). Modeling studies indicate that a cool tropical Pacific combined with a warm North Atlantic is linked with sustained Great Plains drought (Feng et al., 2008). Persistent drought is associated with soil-moisture feedbacks (Schubert et al., 2004b; Wu and Kinter, 2009).

Sustained La Niña-like conditions during the mid-Holocene in the Pacific (Koutavas, 2006; Conroy et al., 2008; Barron and Anderson, 2011) are consistent with mid-Holocene drought in the NGP. The well dated record from El Junco Crater Lake in the Galápagos Islands (Conroy et al., 2008) reveals striking temporal correspondences with Kettle Lake. Grain-size data as a proxy for past lake levels at El Junco indicate suppressed ENSO variability (i.e. sustained La Niña-like conditions) beginning ~9.0 ka, with increased ENSO variability after ~4.2 ka. These shifts in ENSO variability are remarkably similar to the Kettle Lake mode shifts at 9.25 ka and 4.44 ka, which may indicate linkages with tropical Pacific SST and NGP Holocene climate.

Late Holocene ENSO, PDO, and NAO oscillations are of a higher frequency than the dominant 160-yr periodicity (Brown et al., 2005) evident at Kettle Lake. However, the Holocene record of longer-term ENSO variability suggests that important linkages may exist with lower frequency variations of these oscillations. Thus, while ENSO and SST linkages may explain the decadal- and millennial-scale variations seen in the NGP, the cause of the century-scale variations remains elusive. Solar forcing remains a possibility (e.g. Yu and Ito, 1999).

9. Conclusions

Endogenic carbonate is a sensitive indicator of precipitation. Aragonite responds to solute inflow from groundwater, rather than lake salinity. The Holocene is marked by great variability in moisture, and this variability changes in magnitude through the Holocene. Gypsum in Kettle Lake is detrital, and it occurs during somewhat wetter intervals when shallow saline lakes and playas in the region alternately held water forming gypsum then desiccated, exposing sediment and precipitates to deflation.

A late Pleistocene *Picea* zone extends from the base of the core at ~13 ka to 11.93 ka. With *Picea* percentages of only ~20%, this zone represents open parkland. Although relatively moist conditions prevailed, an aragonite peak and inferred dry interval at ~12.75 ka is coeval with the Clovis culture.

An abrupt switch in the endogenic mineral phase of $CaCO_3$ from calcite to aragonite at 10.73 ka may be a threshold effect due to a gradual increase in salinity and Mg/Ca ratio of lake water and may not represent a dramatic shift in climate. However, this changeover does correspond with a drought event evident as a lapse in endogenic carbonate formation and spike in *Ambrosia* pollen.

The interval from 10.73 ka to 9.25 ka was generally moist, but was punctuated by brief droughts at ~100–300 yr intervals. The number of these droughts is similar to the number of Lake Agassiz strandlines and thus the number of transgression–regression cycles for this period. Although suggestive, establishment of causal connections awaits better dating of Agassiz beaches and better determination of the extents of Agassiz regressions.

Major shifts in climate are evident in both mineral and pollen data at 9.25 ka and 4.44 ka. The 9.25 event correlates with a $\delta^{18}O$ minimum in the Greenland ice cores, desiccation and salinity maxima in other NGP lakes, and a major pulse of drainage from Lake Agassiz. The 9.25 event was an abrupt transition, marked by a pronounced low-aragonite dry interval and multiple slump or turbidite units, which presumably formed at low lake levels. It was the most intense drought of the Holocene. The abruptness of the 9.25 ka transition may be related to the sudden retreat of Lake Agassiz and the elimination of its mesoclimate effect during the Holocene insolation maximum, which thrust the region into an insolation controlled regime. The 8.2 ka event is not remarkable in the Kettle Lake record. A shift in pollen data is also evident at 6.25 ka, but not in the mineral data. This shift does correspond in time with changes at other sites bordering the NGP. The 4.44 ka event is less abrupt than the 9.25 event, but nevertheless appears in both mineral and pollen data. The abrupt change at 9.25 ka vs. the more gradual change in the late Holocene may explain the asymmetric response in vegetation seen along the prairie-forest border, with rapid forest retreat and gradual reinvasion, perhaps aided and hindered by fire respectively. An extraordinary 4.2 ka drought is not evident.

The mid- vs. late Holocene are distinguished by the amplitude of the wet-dry cycles—greater in the mid-Holocene—and by pollen spectra. Although highly variable, weedy taxa, mainly Amaranthaceae and *Ambrosia* are more abundant in the mid-Holocene. Poaceae and *Artemisia* are more abundant during the late Holocene. The abundance of weedy taxa in the mid-Holocene is attributed to repeated drought-induced disturbance. However, the great abundance of *Ambrosia*, which is not particularly drought tolerant, indicates high-frequency variability of precipitation overlaid on the longer-term variability evident in the mineral and pollen data. Specifically, wet summers must have periodically occurred during long-term drought intervals in order for *Ambrosia* to proliferate.

The late Holocene is distinguished by an increase in the amplitude of charcoal accumulation cycles as well as by the appearance, continuous occurrence, and gradual increase in *S. densa*. This ubiquitous NGP cryptogam increases with grazing and increased greatly following European settlement and intensive cattle grazing. Two non-exclusive hypotheses may explain its increasing late Holocene abundance: (1) a trend to cooler climate and (2) increasing bison populations and grazing.

Precipitation variations in the NGP have been linked with Pacific and Atlantic sea-surface temperatures, and mid-Holocene drought in the NGP has been linked with sustained La Niña-like conditions in the Pacific. These linkages may explain the decadal- and millennial-scale variations seen in the NGP, but the cause of prominent century-scale variations remains elusive.

Acknowledgments

James S. Clark, George L. Jacobson Jr, Bryan Shuman and Wayne Lusardi assisted with collection of the cores. Jack Renton of WVU shared use of his XRD sample preparation laboratory. We thank Pietra Mueller, Barbara Hansen, and Vania Stefanova for assistance with laboratory work and pollen counting. Jamie West and Sarah Gach aided the tabulation of charcoal. The work benefited from extended discussions with and common interest of a number of colleagues: Jim Almendinger, James Clark, Dan Engstrom, Sheri Fritz, Emi Ito, Mark Shapley and Alison Smith. We also thank two anonymous reviewers for constructive suggestions. This work was funded by the National Science Foundation under Grants ATM-0214108 (to JJD) and ATM-0213246 (to ECG).

Appendix. Supplementary material

Supplementary data associated with this article can be found, in the online version, at doi:10.1016/j.quascirev.2011.05.015.

References

Albertson, F.W., Tomanek, G.W., 1965. Vegetation changes during a 30-year period in grassland communities near Hays, Kansas. Ecology 46, 714–720.

Alley, R.B., Ágústsdóttir, A.M., 2005. The 8k event: cause and consequences of a major Holocene abrupt climate change. Quaternary Science Reviews 24, 1123–1149.

Angiosperm Phylogeny Group, 2009. An update of the Angiosperm Phylogeny Group classification for the orders and families of flowering plants: APG III. Botanical Journal of the Linnean Society 161, 105–121.

Antevs, E., 1955. Geologic-climatic dating in the West. American Antiquity 20, 317–335.

Artz, J.A., 1995. Geological contexts of the early and middle Holocene archaeological record in North Dakota and adjoining areas of the Northern Plains. Special Paper 297. In: BettisIII, E.A. (Ed.), Archaeological Geology of the Archaic Period in North America. Geological Society of America, Boulder, pp. 67–86.

Barlow, M., Nigam, S., Berbery, E.H., 2001. ENSO, Pacific decadal variability, and U.S. summertime precipitation, drought, and stream flow. Journal of Climate 14, 2105–2128.

Barron, J.A., Anderson, L., 2011. Enhanced late Holocene ENSO/PDO expression along the margins of the eastern North Pacific. Quaternary International 235, 3–12.

Becker, A., Ferry, M., Monecke, K., Schnellmann, M., Giardini, D., 2005. Multiarchive paleoseismic record of late Pleistocene and Holocene strong earthquakes in Switzerland. Tectonophysics 400, 153–177.

Bennett, K.D., 1986. Coherent slumping of early postglacial lake sediments at Hall Lake, Ontario, Canada. Boreas 15, 209–215.

Bernabo, J.C., Webb III, T., 1977. Changing patterns in the Holocene pollen record of northeastern North America: a mapped summary. Quaternary Research 8, 64–96.

Bluemle, J.P., Reid, J.R., Mitchell, K.J.R., 2004. Glaciation of North Dakota, U.S.A. In: Ehlers, J., Gibbard, P.L. (Eds.), Quaternary Glaciations – Extent and Chronology, Part II: North America. Developments in Quaternary Science, Part 2, vol. 2. Elsevier, Amsterdam, pp. 207–212.

Booth, R.K., Jackson, S.T., Forman, S.L., Kutzbach, J.E., Bettis III, E.A., Kreig, J., Wright, D.K., 2005. A severe centennial-scale drought in mid-continental North America 4200 years ago and apparent global linkages. The Holocene 15, 321–328.

Bowler, J.M., Teller, J.T., 1986. Quaternary evaporites and hydrological changes, Lake Tyrrell, North–West Victoria. Australian Journal of Earth Sciences 33, 43–63.

Brown, K.J., Clark, J.S., Grimm, E.C., Donovan, J.J., Mueller, P.G., Hansen, B.C.S., Stefanova, I., 2005. Fire cycles in North American interior grasslands and their

relation to prairie drought. Proceedings of the National Academy of Sciences of the United States of America 102, 8865–8870.
Buck, C.E., Christen, J.A., James, G.N., 1999. BCal: an on-line Bayesian radiocarbon calibration tool. Internet Archaeology 7.
Bunkers, M.J., Miller Jr., J.R., DeGaetano, A.T., 1996. An examination of El Niño–La Niña-related precipitation and temperature anomalies across the Northern Plains. Journal of Climate 9, 147–160.
Came, R.E., Oppo, D.W., McManus, J.F., 2007. Amplitude and timing of temperature and salinity variability in the subpolar North Atlantic over the past 10 k.y. Geology 35, 315–318.
Castro, C.L., McKee, T.B., Pielke, R.A., Sr, 2001. The relationship of the North American monsoon to tropical and North Pacific sea surface temperatures as revealed by observational analyses. Journal of Climate 14, 4449–4473.
Chung, F.H., 1974. Quantitative interpretation of X-ray diffraction patterns. I. Matrix-flushing method of quantitative multicomponent analysis. Journal of Applied Crystallography 7, 519–525.
Clark, J.S., Grimm, E.C., Donovan, J.J., Fritz, S.C., Engstrom, D.R., Almendinger, J.E., 2002. Drought cycles and landscape responses to past aridity on prairies of the northern Great Plains, USA. Ecology 83, 595–601.
Clark, J.S., Grimm, E.C., Lynch, J., Mueller, P.G., 2001. Effects of Holocene climate change on the C_4 grassland/woodland boundary in the northern plains, USA. Ecology 82, 620–636.
Clarke, S.E., Tisdale, E.W., Skoglund, N.A., 1943. The Effects of Climate and Grazing Practices on Short-Grass Prairie Vegetation. Publication 747, Technical Bulletin 46. Canada Department of Agriculture.
Clayton, L., Moran, S.R., 1982. Chronology of late Wisconsinan glaciation in middle North America. Quaternary Science Reviews 1, 55–82.
Clayton, L., Moran, S.R., Bickley Jr., W.B., 1976. Stratigraphy, Origin, and Climatic Implications of Late Quaternary Upland Silt in North Dakota. Miscellaneous Series, vol. 54. North Dakota Geological Survey.
Clayton, L., Moran, S.R., Bluemle, J.P., 1980. Explanatory Text to Accompany the Geologic Map of North Dakota. Report of Investigations 69. North Dakota Geological Survey.
COHMAP Members, 1988. Climatic changes of the last 18,000 years: observations and model simulations. Science 241, 1043–1052.
Conroy, J.L., Overpeck, J.T., Cole, J.E., Shanahan, T.M., Steinitz-Kannan, M., 2008. Holocene changes in eastern tropical Pacific climate inferred from a Galápagos lake sediment record. Quaternary Science Reviews 27, 1166–1180.
Coupland, R.T., 1950. Ecology of mixed Prairie in Canada. Ecological Monographs 20, 271–315.
Coupland, R.T., 1992. Mixed Prairie. In: Coupland, R.T. (Ed.), Natural Grasslands: Introduction and Western Hemisphere. Ecosystems of the World, vol. 8A. Elsevier, Amsterdam, pp. 151–182.
Craine, J.M., McLauchlan, K.K., 2004. The influence of biotic drivers on North American palaeorecords: alternatives to climate. The Holocene 14, 787–791.
De Choudens-Sánchez, V., González, L.A., 2009. Calcite and aragonte precipitation under controlled instantaneous supersaturation: elucidating the role of $CaCO_3$ saturation state and Mg/Ca ratio on calcium carbonate polymorphism. Journal of Sedimentary Research 79, 363–376.
Dean Jr., W.E., 1974. Determination of carbonate and organic matter in calcareous sediments and sedimentary rocks by loss on ignition: comparison with other methods. Journal of Sedimentary Petrology 44, 242–248.
Donovan, J.J., Engstrom, D.R., Almendinger, J., Fritz, S., 1999. Endogenic lacustrine carbonate flux as a proxy for paleorecharge; comparing the record of two evaporative groundwater-dominated lakes. Geological Society of America Abstracts with Programs 31 (7), 88.
Donovan, J.J., Grimm, E.C., 2007. Episodic struvite deposits in a northern Great Plains flyway lake: indicators of mid-Holocene drought? The Holocene 17, 1155–1169.
Dorale, J.A., Wozniak, L.A., Bettis III, E.A., Carpenter, S.J., Mandel, R.D., Hajic, E.R., Lopinot, N.H., Ray, J.H., 2010. Isotopic evidence for younger Dryas aridity in the North American midcontinent. Geology 38, 519–522.
Engstrom, D.R., Nelson, S.R., 1991. Paleosalinity from trace metals in fossil ostracodes compared with observational records at Devils Lake, North Dakota, USA. Palaeogeography, Palaeoclimatology, Palaeoecology 83, 295–312.
Fægri, K., Iversen, J., Kaland, P.E., Krzywinski, K., 1989. Textbook of Pollen Analysis, fourth ed. John Wiley & Sons, Chichester.
Feng, S., Oglesby, R.J., Rowe, C.M., Loope, D.B., Hu, Q., 2008. Atlantic and Pacific SST influences on medieval drought in North America simulated by the Community atmospheric model. Journal of Geophysical Research 113, D11101.
Fenton, M.M., Moran, S.R., Teller, J.T., Clayton, L., 1983. Quaternary stratigraphy and history in the southern part of the Lake Agassiz basin. In: Teller, J.T., Clayton, L. (Eds.), Glacial Lake Agassiz. Special Paper 26, Geological Association of Canada, St. John's, pp. 49–74.
Fisher, T.G., Yansa, C.H., Lowell, T.V., Lepper, K., Hajdas, I., Ashworth, A., 2008. The chronology, climate, and confusion of the Moorhead phase of glacial Lake Agassiz: new results from the Ojata beach, North Dakota, USA. Quaternary Science Reviews 27, 1124–1135.
Fleitmann, D., Mudelsee, M., Burns, S.J., Bradley, R.S., Kramers, J., Matter, A., 2008. Evidence for a widespread climatic anomaly at around 9.2 ka before present. Paleoceanography 23, PA1102.
Flora of North America Editorial Committee, 1993+. Flora of North America North of Mexico. Oxford University Press, New York.
Folk, R.L., 1974. The natural history of crystalline calcium carbonate: effect of magnesium content and salinity. Journal of Sedimentary Petrology 44, 40–53.
Forman, S.L., Marín, L., Pierson, J., Gómez, J., Miller, G.H., Webb, R.S., 2005. Aeolian sand depositional records from western Nebraska: landscape response to droughts in the past 1500 years. The Holocene 15, 973–981.
Forman, S.L., Oglesby, R., Webb, R.S., 2001. Temporal and spatial patterns of Holocene dune activity on the Great Plains of North America: megadroughts and climate links. Global and Planetary Change 29, 1–29.
Freers, T.F., 1970. Geology and Ground Water Resources: Williams County, North Dakota. Part I – Geology. Bulletin 48. North Dakota Geological Survey.
Fritz, S.C., 1996. Paleolimnological records of climatic change in North America. Limnology and Oceanography 41, 882–889.
Fritz, S.C., Engstrom, D.R., Haskell, B.J., 1994. 'Little Ice Age' aridity in the northern American Great Plains: a high-resolution reconstruction of salinity fluctuations from Devils Lake, North Dakota, USA. The Holocene 4, 69–73.
Fritz, S.C., Ito, E., Yu, Z., Laird, K.R., Engstrom, D.R., 2000. Hydrologic variation in the Northern Great Plains during the last two millennia. Quaternary Research 53, 175–184.
Fritz, S.C., Juggins, S., Battarbee, R.W., Engstrom, D.R., 1991. Reconstruction of past changes in salinity and climate using a diatom-based transfer function. Nature 352, 706–708.
Gleason, H.A., 1922. The vegetational history of the Middle West. Annals of the Association of American Geographers 12, 39–85.
Gonzales, L.M., Grimm, E.C., 2009. Synchronization of late-glacial vegetation changes at Crystal Lake, Illinois, USA with the North Atlantic event stratigraphy. Quaternary Research 72, 234–245.
Gonzales, L.M., Williams, J.W., Grimm, E.C., 2009. Expanded response-surfaces: a new method to reconstruct paleoclimates from fossil pollen assemblages that lack modern analogues. Quaternary Science Reviews 28, 3315–3332.
Grimm, E.C., 1987. CONISS: a FORTRAN 77 program for stratigraphically constrained cluster analysis by the method of incremental sum of squares. Computers & Geosciences 13, 13–35.
Grimm, E.C., 2001. Trends and palaeoecological problems in the vegetation and climate history of the Northern Great Plains, U.S.A. Biology and Environment: Proceedings of the Royal Irish Academy 101B, 47–64.
Grimm, E.C., 2011. High-resolution age model based on AMS radiocarbon ages for Kettle Lake, North Dakota, USA. Radiocarbon 53, 39–53.
Grimm, E.C., Maher Jr., L.J., Nelson, D.M., 2009. The magnitude of error in conventional bulk-sediment radiocarbon dates from central North America. Quaternary Research 72, 301–308.
Hall-Beyer, M., Gwyn, Q.H.J., 1996. *Selaginella densa* reflectance: relevance to rangeland remote sensing. Journal of Range Management 49, 470–473.
Hansen, D.E., 1967. Geology and Ground Water Resources: Divide County, North Dakota. Part I – Geology. Bulletin 45. North Dakota Geological Survey.
Haskell, B.J., Engstrom, D.R., Fritz, S.C., 1996. Late Quaternary paleohydrology in the North American Great Plains inferred from the geochemistry of endogenic carbonate and fossil ostracodes from Devils Lake, North Dakota, USA. Palaeogeography, Palaeoclimatology, Palaeoecology 124, 179–193.
Haynes Jr., C.V., 1991. Geoarchaeological and paleohydrological evidence for a Clovis-age drought in North America and its bearing on extinction. Quaternary Research 35, 438–450.
Haynes Jr., C.V., 2008. Younger Dryas "black mats" and the Rancholabrean termination in North America. Proceedings of the National Academy of Sciences of the United States of America 105, 6520–6525.
Holliday, V.T., 2000. Folsom drought and episodic drying on the Southern High Plains from 10,900–10,200 ^{14}C yr B.P. Quaternary Research 53, 1–12.
Hostetler, S.W., Bartlein, P.J., Clark, P.U., Small, E.E., Solomon, A.M., 2000. Simulated influences of Lake Agassiz on the climate of central North America 11,000 years ago. Nature 405, 334–337.
Howard, A.D., 1958. Drainage evolution in northeastern Montana and northwestern North Dakota. Geological Society of America Bulletin 69, 575–588.
Hubbard, W.A., 1951. Rotational grazing studies in western Canada. Journal of Range Management 4, 25–29.
Jacobson Jr., G.L., Grimm, E.C., 1986. A numerical analysis of Holocene forest and prairie vegetation in central Minnesota. Ecology 67, 958–966.
Jones, B.F., Bowser, C.J., 1978. The mineralogy and related chemistry of lake sediments. In: Lerman, A. (Ed.), Lakes: Chemistry, Geology, Physics. Springer-Verlag, New York.
Kelts, K., Hsü, K.J., 1978. Freshwater carbonate sedimentation. In: Lerman, A. (Ed.), Lakes: Chemistry, Geology, Physics. Springer-Verlag, New York, pp. 294–323.
Kennedy, K.A., 1994. Early-Holocene geochemical evolution of saline Medicine Lake, South Dakota. Journal of Paleolimnology 10, 69–84.
Koutavas, A., deMenocal, P.B., Olive , Lynch-Stieglitz, J, G.C., 2006. Mid-Holocene El Niño–Southern Oscillation (ENSO) attenuation revealed by individual foraminifera in eastern tropical Pacific sediments. Geology 34, 993–996.
Laird, K.R., Cumming, B.F., Wunsam, S., Rusak, J.A., Oglesby, R.J., Fritz, S.C., Leavitt, P.R., 2003. Lake sediments record large-scale shifts in moisture regimes across the northern prairies in North America during the past two millennia. Proceedings of the National Academy of Sciences of the United States of America 100, 2483–2488.
Laird, K.R., Fritz, S.C., Cumming, B.F., 1998a. A diatom-based reconstruction of drought intensity, duration, and frequency from Moon Lake, North Dakota: a sub-decadal scale record of the last 2300 years. Journal of Paleolimnology 19, 161–179.
Laird, K.R., Fritz, S.C., Cumming, B.F., Grimm, E.C., 1998b. Early-Holocene limnological and climatic variability in the northern Great Plains. The Holocene 8, 275–285.

Laird, K.R., Fritz, S.C., Grimm, E.C., Mueller, P.G., 1996a. Century-scale paleoclimatic reconstruction from Moon Lake, a closed-basin lake in the northern Great Plains. Limnology and Oceanography 41, 890–902.

Laird, K.R., Fritz, S.C., Maasch, K.A., Cumming, B.F., 1996b. Greater drought intensity and frequency before AD 1200 in the Northern Great Plains, USA. Nature 384, 552–554.

Laird, K.R., Michels, A., Stuart, C.T.L., Wilson, S.E., Last, W.M., Cumming, B.F., 2007. Examination of diatom-based changes from a climatically sensitive prairie lake (Saskatchewan, Canada) at different temporal perspectives. Quaternary Science Reviews 26, 3328–3343.

Larsen, G., Chilingar, G.V., (Eds.), 1967. Diagenesis in Sediments. Developments in Sedimentology, vol. 8. Elsevier, Amsterdam.

Larson, G.E., 1993. Aquatic and Wetland Vascular Plants of the Nnorthern Great Plains. General Technical Report RM-238. United States Deparatment of Agriculture, Forest Service, Rocky Mountain Forest and Range Experiment Station, Fort Collins.

Last, W.M., 1984. Sedimentology of playa lakes of the Northern Great Plains. Canadian Journal of Earth Sciences 21, 107–125.

Last, W.M., 1993. Geolimnology of FreefightLake: an unusual hypersaline lake in the northern Great Plains of western Canada. Sedimentology 40, 431–448.

Last, W.M., 2001. Mineralogical analysis of lake sediments. In: Last, W.M., Smol, J.P. (Eds.), Tracking Environmental Change Using Lake Sediments. Physical and Geochemical Methods, vol. 2. Kluwer Academic Publishers, Dordrecht.

Last, W.M., 2002. Geolimnology of salt lakes. Geosciences Journal 6, 347–369.

Last, W.M., Deleqiat, J., Greengrass, K., Sukhan, S., 2002. Re-examination of the recent history of meromictic Waldsea Lake, Saskatchewan, Canada. Sedimentary Geology 148, 147–160.

Last, W.M., Ginn, F.M., 2005. Saline systems of the Great Plains of Western Canada: an overview of the limnogeology and paleolimnology. Saline Systems 1, 10.

Last, W.M., Sauchyn, D.J., 1993. Mineralogy and lithostratigraphy of Harris Lake, Southwestern Saskatchewan, Canada. Journal of Paleolimnology 9, 23–39.

Last, W.M., Vance, R.E., 2002. The Holocene history of Oro Lake, one of the western Canada's longest continuous lacustrine records. Sedimentary Geology 148, 161–184.

Last, W.M., Vance, R.E., Wilson, S., Smol, J.P., 1998. A multi-proxy limnologic record of rapid early-Holocene hydrologic change on the northern Great Plains, southwestern Saskatchewan, Canada. The Holocene 8, 503–520.

Lauenroth, W.K., Sala, O.E., 1992. Long-term forage production of North American shortgrass steppe. Ecological Applications 2, 397–403.

Lauenroth, W.K., Whitman, W.C., 1977. Dynamics of dry matter production in a mixed-grass prairie in western North Dakota. Oecologia 27, 339–351.

Lepper, K., Fisher, T.G., Hajdas, I., Lowell, T.V., 2007. Ages for the Big Stone Moraine and the oldest beaches of glacial Lake Agassiz: implications for deglaciation chronology. Geology 35, 667–670.

Leverington, D.W., Mann, J.D., Teller, J.T., 2002. Changes in the bathymetry and volume of glacial Lake Agassiz between 9200 and 7700 ^{14}C yr B.P. Quaternary Research 57, 244–252.

Leverington, D.W., Teller, J.T., 2003. Paleotopographic reconstructions of the eastern outlets of glacial Lake Agassiz. Canadian Journal of Earth Sciences 40, 1259–1278.

Lowe, J.J., Rasmussen, S.O., Björck, S., Hoek, W.Z., Steffensen, J.P., Walker, M.J.C., Yu, Z.C., INTIMATE group, 2008. Synchronisation of palaeoenvironmental events in the North Atlantic region during the Last Termination: a revised protocol recommended by the INTIMATE group. Quaternary Science Reviews 27, 6–17.

Marshall, J.D., Lang, B., Crowley, S.F., Weedon, G.P., van Calsteren, P., Fisher, E.H., Holme, R., Holmes, J.A., Jones, R.T., Bedford, A., Brooks, S.J., Bloemendal, J., Kiriakoulakis, K., Ball, J.D., 2007. Terrestrial impact of abrupt changes in the North Atlantic thermohaline circulation: early Holocene, UK. Geology 35, 639–642.

Mason, J.A., Miao, X., Hanson, P.R., Johnson, W.C., Jacobs, P.M., Goble, R.J., 2008. Loess record of the Pleistocene-Holocene transition on the northern and central Great Plains, USA. Quaternary Science Reviews 27, 1772–1783.

McAndrews, J.H., 1966. Postglacial history of prairie, savanna, and forest in northwestern Minnesota. Torrey Botanical Club Memoir 22 (2), 1–72.

McDonald, J.N., 1981. North American Bison: Their Classification and Evolution. University of California Press, Berkeley.

Miao, X., Mason, J.A., Goble, R.J., Hanson, P.R., 2005. Loess record of dry climate and aeolian activity in the early- to mid-Holocene, central Great Plains, North America. The Holocene 15, 339–346.

Miao, X., Mason, J.A., Swinehart, J.B., Loope, D.B., Hanson, P.R., Goble, R.J., Liu, X., 2007. A 10,000 year record of dune activity, dust storms, and severe drought in the central Great Plains. Geology 35, 119–122.

Mott, R.J., 1973. Palynological Studies in Central Saskatchewan. Paper 72–49. Geological Survey of Canada, Ottawa.

Muhs, D.R., Stafford Jr., T.W., Been, J., Mahan, S.A., Burdett, J., Skipp, G., Rowland, Z.M., 1997. Holocene eolian activity in the Minot dune field, North Dakota. Canadian Journal of Earth Sciences 34, 1442–1459.

Mulder, T., Cochonat, P., 1996. Classification of offshore mass movements. Journal of Sedimentary Research 66, 43–57.

Nelson, D.M., Hu, F.S., 2008. Patterns and drivers of Holocene vegetational change near the prairie–forest ecotone in Minnesota: revisiting McAndrews' transect. New Phytologist 179, 449–459.

Nelson, D.M., Hu, F.S., Grimm, E.C., Curry, B.B., Slate, J.E., 2006. The influence of aridity and fire on Holocene prairie communities in the eastern prairie Peninsula. Ecology 87, 2523–2536.

Pienitz, R., Smol, J.P., Last, W.M., Leavitt, P.R., Cumming, B.F., 2000. Multi-proxy Holocene palaeoclimatic record from a saline lake in the Canadian subarctic. The Holocene 10, 673–686.

Radle, N.J., 1981. Vegetation History and Lake-level Changes at a Saline Lake in Northeastern South Dakota. Master's Thesis, University of Minnesota, Minneapolis.

Radle, N.J., Keister, C.M., Battarbee, R.W., 1989. Diatom, pollen, and geochemical evidence for the palaeosalinity of Medicine Lake, S. Dakota, during the late Wisconsin and early Holocene. Journal of Paleolimnology 2, 159–172.

Rasmussen, S.O., Vinther, B.M., Clausen, H.B., Andersen, K.K., 2007. Early Holocene climate oscillations recorded in three Greenland ice cores. Quaternary Science Reviews 26, 1907–1914.

Reimer, P.J., Baillie, M.G.L., Bard, E., Bayliss, A., Beck, J.W., Blackwell, P.G., Ramsey, C.B., Buck, C.E., Burr, G.S., Edwards, R.L., Friedrich, M., Grootes, P.M., Guilderson, T.P., Hajdas, I., Heaton, T.J., Hogg, A.G., Hughen, K.A., Kaiser, K.F., Kromer, B., McCormac, F.G., Manning, S.W., Reimer, R.W., Richards, D.A., Southon, J.R., Talamo, S., Turney, C.S.M., van der Plicht, J., Weyhenmeyer, C.E., 2009. IntCal09 and Marine09 radiocarbon age calibration curves, 0–50,000 years cal BP. Radiocarbon 51, 1111–1150.

Ritchie, J.C., 1964. Contributions to the Holocene paleoecology of westcentral Canada I. The riding mountain area. Canadian Journal of Botany 42, 181–196.

Ritchie, J.C., 1976. The late-Quaternary vegetational history of the western interior of Canada. Canadian Journal of Botany 54, 1793–1818.

Ritchie, J.C., Lichti-Federovich, S., 1968. Holocene pollen assemblages from the Tiger Hills, Manitoba. Canadian Journal of Earth Sciences 5, 873–880.

Rogler, G.A., Hass, H.J., 1956. Range production as related to soil moisture and precipitation on the Northern Great Plains. Journal of the American Society of Agronomy 39, 378–389.

Rohling, E.J., Pälike, H., 2005. Centennial-scale climate cooling with a sudden cold event around 8,200 years ago. Nature 434.

Ruiz-Barradas, A., Nigam, S., 2005. Warm season rainfall variability over the U.S. Great Plains in observations, NCEP and ERA-40 reanalyses, and NCAR and NASA atmospheric model simulations. Journal of Climate 18, 1808–1830.

Sack, L.A., Last, W.M., 1994. Lithostratigraphy and recent sedimentation history of Little Manitou Lake, Saskatchewan, Canada. Journal of Paleolimnology 10, 199–212.

Schnurrenberger, D., Russell, J., Kelts, K., 2003. Classification of lacustrine sediments based on sedimentary components. Journal of Paleolimnology 29, 141–154.

Schubert, S.D., Suarez, M.J., Pegion, P.J., Koster, R.D., Bacmeister, J.T., 2004a. Causes of long-term drought in the U.S. Great Plains. Journal of Climate 17, 485–503.

Schubert, S.D., Suarez, M.J., Pegion, P.J., Koster, R.D., Bacmeister, J.T., 2004b. On the cause of the 1930s dust bowl. Science 303, 1855–1859.

Schubert, S.D., Suarez, M.J., Pegion, P.J., Koster, R.D., Bacmeister, J.T., 2008. Potential predictability of long-term drought and pluvial conditions in the U.S. Great Plains. Journal of Climate 21, 802–816.

Seager, R., Kushnir, Y., Herweijer, C., Naik, N., Velez, J., 2005. Modeling of tropical forcing of persistent droughts and pluvials over western North America: 1856–2000. Journal of Climate 18, 4065–4088.

Seilacher, A., 1984. Sedimentary structures tentatively attributed to seismic events. Marine Geology 55, 1–12.

Shao, X., Wang, Y., Cheng, H., Kong, X., Wu, J., Edwards, R.L., 2006. Long-term trend and abrupt events of the Holocene Asian monsoon inferred from a stalagmite δ^{18}O record from Shennongjia in Central China. Chinese Science Bulletin 51, 221–228.

Shapley, M.D., Ito, E., Donovan, J.J., 2005. Authigenic calcium carbonate flux in groundwater-controlled lakes: implications for lacustrine paleoclimate records. Geochimica et Cosmochimica Acta 69, 2517–2533.

Shapley, M.D., Ito, E., Forester, R.M., 2010. Negative correlations between Mg:Ca and total dissolved solids in lakes: false aridity signals and decoupling mechanism for paleohydrologic proxies. Geology 38, 427–430.

Singh, J.S., Lauenroth, W.K., Heitschmidt, P.K., Dodd, J.L., 1983. Structural and functional attributes of the vegetation of northern mixed prairie of North America. Botanical Review 49, 117–149.

Smith, A.J., Donovan, J.J., Ito, E., Engstrom, D.R., Panek, V.A., 2002. Climate-driven hydrologic transients in lake sediment records: multiproxy record of mid-Holocene drought. Quaternary Science Reviews 21, 625–646.

Smoliak, S., 1960. Effects of deferred-rotation and continuous grazing on yearling steer gains and shortgrass prairie vegetation of southeastern Alberta. Journal of Range Management 13, 239–243.

Smoliak, S., 1965. A comparison of ungrazed and lightly grazed *Stipa-Bouteloua* prairie in southeastern Alberta. Canadian Journal of Plant Science 45, 270–275.

Smoliak, S., 1986. Influence of climatic conditions on production of *Stipa-Bouteloua* prairie over a 50-year period. Journal of Range Management 39, 100–103.

Stevens, P.F., 2001, onwards. Angiosperm Phylogeny Website. Version 9, June 2008. http://www.mobot.org/MOBOT/research/APweb.

Stubbendieck, J., Friisoe, G.Y., Bolick, M.R., 1995. Weeds of Nebraska and the Great Plains, second ed. Nebraska Department of Agriculture, Lincoln.

Stuiver, M., Reimer, P.J., 1993. Extended ^{14}C database and revised CALIB radiocarbon calibration program. Radiocarbon 35, 215–230.

Taylor, J.E., Lacey, J.R., 1994. Range Plants of Montana. Extension Bulletin 122. Montana State University Extension Service, Bozeman.

Teed, R., Umbanhowar, C., Camill, P., 2009. Multiproxy lake sediment records at the northern and southern boundaries of the Aspen Parkland region of Manitoba, Canada. The Holocene 19, 937–948.

Teller, J.T., Leverington, D.W., 2004. Glacial Lake Agassiz: a 5000 yr history of change and its relationship to the $\delta^{18}O$ record of Greenland. Geological Society of America Bulletin 116, 729–742.

Teller, J.T., Leverington, D.W., Mann, J.D., 2002. Freshwater outbursts to the oceans from glacial Lake Agassiz and their role in climate change during the last deglaciation. Quaternary Science Reviews 21, 879–887.

Till, R., Spears, D.A., 1969. The determination of quartz in sedimentary rocks using an X-ray diffraction method. Clays and Clay Minerals 17, 323–329.

Ting, M., Wang, H., 1997. Summertime U.S. precipitation variability and its relation to Pacific sea surface temperature. Journal of Climate 10, 1853–1873.

Umbanhowar Jr., C.E., 2004. Interactions of climate and fire at two sites in the northern Great Plains, USA. Palaeogeography, Palaeoclimatology, Palaeoecology 208, 141–152.

Umbanhowar Jr., C.E., Camill, P., Geiss, C.E., Teed, R., 2006. Asymmetric vegetation responses to mid-Holocene aridity at the prairie-forest ecotone in South–Central Minnesota. Quaternary Research 66, 53–66.

Valdespino, I.A., 1993. Selaginellaceae Willkomm: spike-moss family. In: Flora of North America Editorial Committee (Ed.), Flora of North America North of Mexico, vol. 2. Oxford University Press, New York, pp. 38–63.

Valero-Garcés, B.L., Kelts, K.R., 1995. A sedimentary facies model for perennial and meromictic saline lakes: Holocene Medicine Lake basin, South Dakota, USA. Journal of Paleolimnology 14, 123–149.

Valero-Garcés, B.L., Laird, K.R., Fritz, S.C., Kelts, K., Ito, E., Grimm, E.C., 1997. Holocene climate in the northern Great Plains inferred from sediment stratigraphy, stable isotopes, carbonate geochemistry, diatoms, and pollen at Moon Lake, North Dakota. Quaternary Research 48, 359–369.

Van Zant, K.L., 1979. Late glacial and postglacial pollen and plant macrofossils from Lake West Okoboji, northwestern Iowa. Quaternary Research 12, 358–380.

Vance, R.E., Clague, J.J., Mathewes, R.W., 1993. Holocene paleohydrology of a hypersaline lake in Southeastern Alberta. Journal of Paleolimnology 8, 103–120.

Vance, R.E., Mathewes, R.W., Clague, J.J., 1992. 7000 year record of lake-level change on the northern Great Plains: a high-resolution proxy of past climate. Geology 20, 879–882.

Vinther, B.M., Clausen, H.B., Johnsen, S.J., Rasmussen, S.O., Andersen, K.K., Buchardt, S.L., Dahl-Jensen, D., Seierstad, I.K., Siggaard-Andersen, M.-L., Steffensen, J.P., Svensson, A., Olsen, J., Heinemeier, J., 2006. A synchronized dating of three Greenland ice cores throughout the Holocene. Journal of Geophysical Research 111, D13102.

Waters, M.R., Stafford Jr., T.W., 2007. Redefining the age of Clovis: implications for the peopling of the Americas. Science 315, 1122–1126.

Watts, W.A., Bright, R.C., 1968. Pollen, seed, and mollusk analysis of a sediment core from Pickerel Lake, northeastern South Dakota. Geological Society of America Bulletin 79, 855–876.

Weaver, J.E., 1968. Prairie Plants and Their Environment: A Fifty-year Study in the Midwest. University of Nebraska Press, Lincoln.

Weaver, J.E., Albertson, F.W., 1936. Effects of the great drought on the prairies of Iowa, Nebraska, and Kansas. Ecology 17, 567–639.

Weaver, J.E., Albertson, F.W., 1956. Grasslands of the Great Plains: Their Nature and Use. Johnsen Publishing Company, Lincoln.

Weaver, S.J., Nigam, S., 2008. Variability of the Great Plains low-level jet: large-scale circulation context and hydroclimate impacts. Journal of Climate 21, 1532–1551.

Webb III, T., Cushing, E.J., Wright Jr., H.E., 1983. Holocene changes in the vegetation of the Midwest. In: Wright Jr., H.E. (Ed.), The Holocene. Late-Quaternary Environments of the United States. University of Minnesota Press, Minneapolis, pp. 142–165.

Webster, T.R., Steeves, T.A., 1964. Observations on drought resistance in *Selaginella densa* Rydb. American Fern Journal 54, 189–196.

Whitman, W.C., Wali, M.K., 1975. Grasslands of North Dakota. In: Wali, M.K. (Ed.), Prairie: A Multiple View. University of North Dakota Press, Grand Forks, pp. 53–73.

Williams, J.W., Shuman, B., Bartlein, P.J., 2009. Rapid responses of the prairie-forest ecotone to early Holocene aridity in mid-continental North America. Global and Planetary Change 66, 195–207.

Williams, J.W., Shuman, B., Bartlein, P.J., Whitmore, J., Gajewski, K., Sawada, M., Minckley, T., Shafer, S., Viau, A.E., Webb III, T., Anderson, P., Brubaker, L., Whitlock, C., Davis, O.K., 2006. An Atlas of Pollen-vegetation-climate Relationships for the United States and Canada. In: Contribution Series, vol. 43. American Association of Stratigraphic Palynologists, Dallas.

Winter, T.C., Rosenberry, D.O., 1995. The interaction of ground water with prairie pothole wetlands in the Cottonwood Lake area, East–Central North Dakota, 1979–1990. Wetlands 15, 193–211.

Witkind, I.J., 1959. Quaternary Geology of the Smoke Creek-Medicine Lake-Grenora Area, Montana and North Dakota. Bulletin 1073. United States Geological Survey.

Wolfe, S.A., Muhs, D.R., David, P.P., McGeehin, J.P., 2000. Chronology and geochemistry of late Holocene eolian deposits in the Brandon sand Hills, Manitoba, Canada. Quaternary International 67, 61–74.

Wolfe, S.A., Ollerhead, J., Lian, O.B., 2002. Holocene eolian activity in South–Central Saskatchewan and the southern Canadian prairies. Géographie physique et Quaternaire 56, 215–227.

Woodhouse, C.A., Overpeck, J.T., 1998. 2000 years of drought variability in the central United States. Bulletin of the American Meteorological Society 79, 2693–2714.

Wright Jr., H.E., Mann, D.H., Glaser, P.H., 1984. Piston corers for peat and lake sediments. Ecology 65, 657–659.

Wright Jr., H.E., Stefanova, I., Tian, J., Brown, T.A., Hu, F.S., 2004. A chronological framework for the Holocene vegetational history of central Minnesota: the Steel Lake pollen record. Quaternary Science Reviews 23, 611–626.

Wright Jr., H.E., Winter, T.C., Patten, H.L., 1963. Two pollen diagrams from southeastern Minnesota: problems in the regional late-glacial and postglacial vegetational history. Geological Society of America Bulletin 74, 1371–1396.

Wu, R., Kinter III, J.L., 2009. Analysis of the relationship of U.S. droughts with SST and soil moisture: distinguishing the time scale of droughts. Journal of Climate 22, 4520–4538.

Yansa, C.H., 1998. Holocene paleovegetation and paleohydrology of a prairie pothole in Southern Saskatchewan, Canada. Journal of Paleolimnology 19, 429–441.

Yansa, C.H., 2006. The timing and nature of late Quaternary vegetation changes in the Northern Great Plains, USA and Canada: a re-assessment of the spruce phase. Quaternary Science Reviews 25, 263–281.

Yansa, C.H., Basinger, J.F., 1999. A postglacial plant macrofossil record of vegetation and climate change in southern Saskatchewan. Geological Survey of Canada Bulletin 534, 139–172.

Yansa, C.H., Dean, W.E., Murphy, E.C., 2007. Late Quaternary paleoenvironments of an ephemeral wetland in North Dakota, USA: relative interactions of ground-water hydrology and climate change. Journal of Paleolimnology 38, 441–457.

Yu, S.-Y., Colman, S.M., Lowell, T.V., Milne, G.A., Fisher, T.G., Breckenridge, A., Boyd, M., Teller, J.T., 2010. Freshwater outburst from Lake Superior as a trigger for the cold event 9300 years ago. Science, 1262–1266.

Yu, Z., Ito, E., 1999. Possible solar forcing of century-scale drought frequency in the northern Great Plains. Geology 27, 263–266.

Yu, Z., Ito, E., Engstrom, D.R., Fritz, S.C., 2002. A 2100-year trace-element and stable-isotope record at decadal resolution from Rice Lake in the Northern Great Plains, USA. The Holocene 12, 605–617.

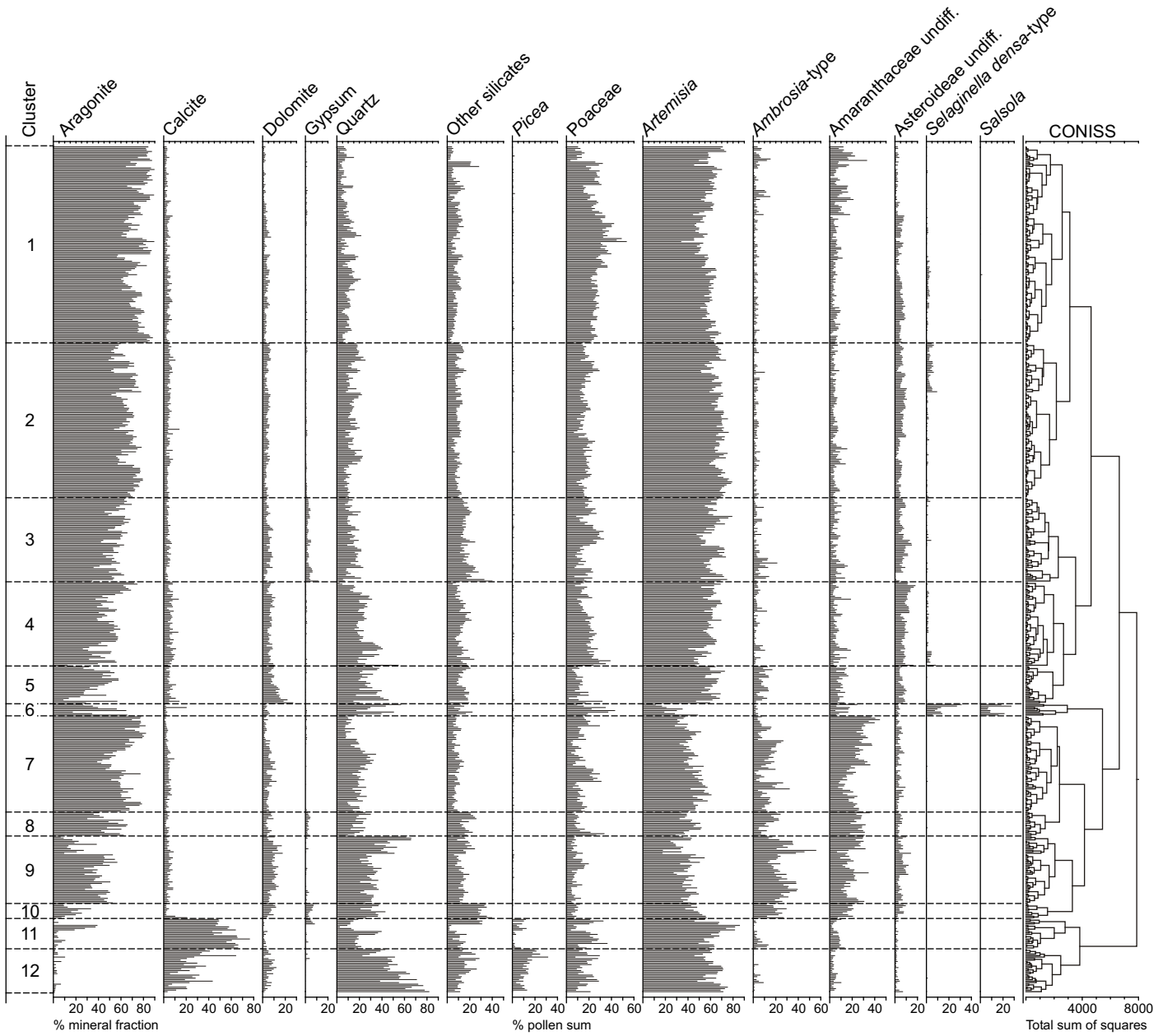

Fig. S1. Results of the stratigraphically unconstrained CONISS cluster analysis of minerals, pollen, and charcoal. Clusters are designated 1–12 on the left side of the diagram.